Structural Engineering and Mechanics, *Vol. 55, No. 3 (2015) 605-638*
DOI: http://dx.doi.org/10.12989/sem.2015.55.3.605

Buckling analysis of semi-rigid gabled frames

Mohammad Rezaiee-Pajand*, Farzad Shahabian[a] and Mohsen Bambaeechee[b]

Department of Civil Engineering, Faculty of Engineering, Ferdowsi University of Mashhad, Iran

(Received April 13, 2014, Revised January 26, 2015, Accepted July 7, 2015)

Abstract. It is intended to perform buckling analysis of steel gabled frames with tapered members and flexible connections. The method is based on the exact solutions of the governing differential equations for stability of a gabled frame with I-section elements. Corresponding buckling load and subsequently effective length factor are obtained for practical use. For several popular frames, the influences of the shape factor, taper ratio, span ratio, flexibility of connections and elastic rotational and translational restraints on the critical load, and corresponding equivalent effective length coefficient are studied. Some of the outcomes are compared against available solutions, demonstrating the accuracy, efficiency and capabilities of the presented approach.

Keywords: gabled frame; tapered member; I-section; flexible connection; critical load; effective length factor; buckling

1. Introduction

Gabled steel portal frames with non-prismatic members are the most commonly steelwork among the structures used in single storey industrial buildings. The members of these constructions are generally made of I-shape plates in two types: with linearly varying amplitudes of web and flanges or web-tapered I-section. Subsequently, the member moment of inertia variation is approximated as cubic and parabolic functions, respectively. It should be added that the tapering for both beams and columns provide a better distribution of structural strength, and they offer a lighter design. This research deals with the buckling analysis of semi-rigid gabled frames consisting of linearly tapered I-section elements. It is reminded that the flexibilities of connections and elastic supports of the frame are modeled by linear springs.

Stability represents a fundamental problem, which must be mastered to ensure the safety of structures against collapse (Bazant 2000). Elastic buckling of end-loaded, tapered, cantilevered beams with initial curvature were investigated by Wilson and Strong (1997). Essa (1998) developed a new approximate method for the determination of effective length factors for columns in unbraced frames. Based on stability theory of rigid steel frames and using the three-column sub-assemblage model, Wang and Li (2007) presented the governing equations for determining the

*Corresponding author, Professor, E-mail: rezaiee@um.ac.ir
[a]Associate Professor, E-mail: shahabf@um.ac.ir
[b]Ph.D. Student, E-mail: mohsen_bambaeechee@yahoo.com

http://www.techno-press.org/?journal=sem&subpage=8 ISSN: 1225-4568 (Print), 1598-6217 (Online)

effective length factor of the columns in semi-rigid composite frames. Recently, Rayleigh-Ritz procedure for determination of the critical load of tapered columns was utilized by Marques *et al*. (2014). The stability analysis and design of the gabled frames have been treated in the past, and still remains an important research topic. Lu (1964) presented a graph to determine the effective length factors of uniform columns for a pin-based, and partially restrain-based gabled frames. Lee *et al*. (1971), Lee and Morrell (1975) proposed recommendations in structural design guide for calculation of effective length coefficients of tapered columns in the gabled frames. Charts for determining effective length factors of gabled frame columns were presented by the AISC standard (AISC 1999). Based on the matrix force method, a program for calculating member sizes to yield a minimum weight gabled frame with tapered members was developed by Miller and Moll (1979). Fraser (1980) presented design-aid information for calculating the effective length factors of prismatic columns in pitched-roof (gabled) frame. Moreover, this investigator, proposed guidelines for design of the gabled frames with tapered members (Fraser 1983). Using the finite element method, Karabalis and Beskos (1983) studied the static, dynamic and stability analyses of structures including gabled frames, composed of tapered members.

Manolis *et al*. (1986) utilized the assumptions of first-order rigid-plastic theory and the principle of virtual work for the elasto-plastic analysis and design of gabled frames. By using the equilibrium and continuity conditions, an approximate method for calculating the critical load of simple portal or gabled steel frames with varying moment of inertia, was proposed by Irani (1988). Simitses and Mohamed (1989) studied the non-linear analysis of gabled frames with linear and non-linear flexible joint connections and elastic rotational restraints. Furthermore, these researchers, investigated the effects of several parameters on the buckling mode and critical load of the gabled frame (Mohamed and Simitses 1989). By using shaking table, the dynamic characteristics of the pinned-base steel gabled frame with prismatic members were obtained by Hwang *et al*. (1989). Rezaiee-Pajand (1990) presented the formulation for calculating end moment of the gabled frame members which are primarily subjected to bending. A non-linear elasto-plastic instability analysis of rigid and flexibly connected gabled frames with uniform and non-uniform members was proposed by Simitses and Mohamed (1990), Mohamed *et al*. (1991, 1992).

Vlahinos and Cervantes (1990) investigated the buckling and post-buckling behavior of planar steel gabled frame under static loading with imperfection. The dynamic responses of a one-fifth-scale gabled frame composed of tapered members subjected to El Centro earthquake ground motions, using shaking table, were obtained by Hwang *et al*. (1991). An algorithm for the optimum design of steel frames including gabled frame with prismatic and tapered I-section members was presented by Hayalioglu and Saka (1992), Saka (1997). Ronagh and Bradford (1996) developed a general finite element method for the analysis of coupled local and lateral buckling of steel structures composed of tapered I-sections. This method is used to investigate the significance of distortion in the buckling of a typical gabled frame under gravity loads. The elastic in-plane buckling, second-order behavior and design of unbraced pitched-roof steel frames with rigid and semi-rigid connections were studied by Silvestre and Camotim (2005, 2007) and Silvestre *et al*. (1998, 2000).

Li and Li (2000, 2002) used the Chebyshev Polynomial Approach for solving the governing equations of a tapered Timoshenko-Euler beam element in the analysis of steel portal frames. Accordingly, static, dynamic and stability responses of individual tapered members and a gabled frame with tapered beam-column were investigated. In another article, these investigators, studied integrated structural designs, with consideration of system readability for steel gabled frames comprising tapered members (Li and Li 2004). Moreover, Li *et al*. (2003) proposed a concentrated

plasticity model for second-order inelastic analysis of the steel frames of tapered members with a slender web and responses compared with the experimental test results of a gabled frame. A power series approach was used by Al-Sadder (2004) for solving the fourth-order ordinary differential equation of a non-prismatic beam-column member with variable coefficients. Advanced analysis of steel portal and gabled frame structures subjected to lateral torsional buckling effects was performed by Yuan (2004). Liao *et al*. (2005) analyzed the effects of the joint flexibility on the steel gabled frames with pinned and fixed bases. A robust finite element procedure for large deflection and inelastic analysis of imperfect portal and gabled steel frames with semi-rigid bases was suggested by Chan *et al*. (2005). They also studied the non-linear behavior of semi-rigid frames with various modes of initial imperfection. Plane steel portal frames with pitched roof and exposed to fire were examined by Papadopoulos *et al*. (2008). Saffari *et al*. (2008) proposed design-oriented charts for quick calculation of the effective length factor of columns in steel gabled frame with tapered members. A prismatic and non-prismatic stiffness matrix solution for haunched-rafter pitched-roof steel portal frames was presented by Issa and Mohammad (2009), based on the virtual work approach.

Safavi and Moharami (2009) obtained the critical load and corresponding effective length coefficient of tapered gabled frame by equating the structural external work to its internal flexural strain energy. Xu *et al*. (2010) studied the effective length factor of tapered gabled portal frames with leaning columns. A new procedure to find the exact shape functions and stiffness matrices of non-prismatic beam elements was obtained by Shooshtari and Khajavi (2010). Accordingly, they studied behavior of gabled frame with non-prismatic Euler-Bernoulli members. Li *et al*. (2011) investigated the in-plane buckling analysis of gabled arch frame steel building using finite element method. Based on the numerical simulations and experimental research, Wang *et al*. (2011), studied the effects of semi-rigid connections in gabled frames. Tajmir Riahi *et al*. (2012) used the slope-deflection method to present a new method for buckling analysis of tapered columns and gabled frames with tapered members. Recently, based on the advanced finite element method, Cristutiu and Nunes (2013a, b) studied the behavior of steel pitched-roof portal frames with tapered web and flange members considering lateral restraint and initial imperfections.

Based on this brief review, it is obvious that no attempt has been made yet for considering the flexibility of connections and supports in buckling analyses of the gabled frames with different I-tapered members. The object of this study is to derive the exact expression for the gabled frame critical load, taking into account the above effects with various I-sections. Finding numerical results, demonstrating the accuracy, efficiency and capabilities of the presented approach, is another goal of this article. Furthermore, the influences of several parameters such as the taper ratio, span ratio, flexibility of connections and elastic supports on the buckling load and corresponding equivalent effective length factor will be investigated. The outcomes obtained herein can be readily applied for the stability design of a semi-rigid gabled frame with tapered members.

2. Stability formulation

In this section, the elastic stability analysis of the gabled frames shown in Figs. 1(a)-(b) will be performed. The frame in Fig. 1(a), has uniform members; while that of Fig. 1(b) is composed of the tapered members. In both of the gabled frames, α is the frame slope. It is assumed that the columns and beams have lengths of l_c and l_b, respectively, and their moments of inertia vary in the

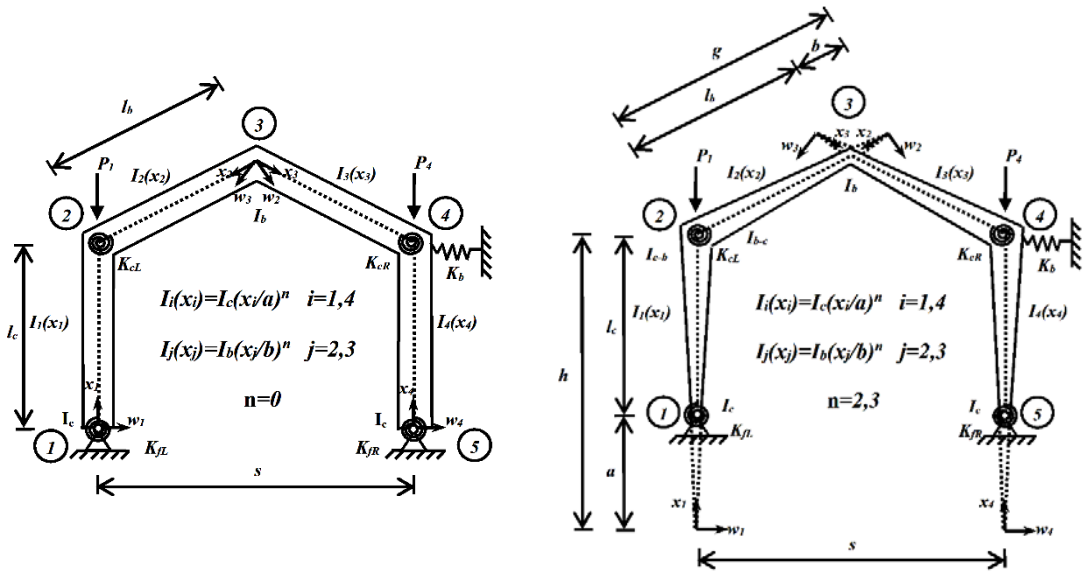

(a) With prismatic members (b) With non-prismatic members

Fig. 1 Geometry and sign convention of gabled frames with flexible supports and connections

following forms:

$$\left.\begin{aligned} I_i(x_i) &= I_c\left(\frac{x_i}{a}\right)^n \qquad (i=1,4) \\ I_j(x_j) &= I_b\left(\frac{x_j}{b}\right)^n \qquad (j=2,3) \end{aligned}\right\} \tag{1}$$

In these functions, a and x_i are distances from the origin for the columns and similarly, b and x_j represent distances from the origin for the beams, as shown in Fig. 1(b). I_c and $I_{c\text{-}b}$ are the moments of inertia at the foundations (i.e., points 1 and 5) and eaves (i.e., points 2 and 4) of the columns, respectively. The beams' moments of inertia at the apex (i.e., point 3) and eaves are I_b and $I_{b\text{-}c}$, respectively. As shown in Fig. 1(b), the moments of inertia of beams and columns for the uniform gabled frame, are I_b and I_c, respectively. Each frame is subjected to two vertical concentrated loads, P_1 and P_4, on the centerline of the columns. It is assumed that the left and right beam-to-column connections, have rotational stiffnesses of K_{cL} and K_{cR}, respectively. The elastic bracing support is modeled by a horizontal spring with translational stiffness K_b, which is located at the top of the right hand side column. Furthermore, the rotational stiffness of elastic supports at the left and right hand side columns are modeled by springs with rotational stiffnesses of K_{fL} and K_{fR}, respectively, which are located at the bases of the columns. The behaviors of all springs are considered to be linear.

In Eq. (1), n is the shape factor and represents the moment of inertia variation along the member length. According to Fig. 2(a), the moment of inertia variation along the length of I-section member, with linearly varying amplitudes for web and flanges, is approximated as cubic function (i.e., n=3). Similarly, based on the Fig. 2(b), the moment of inertia variation along the

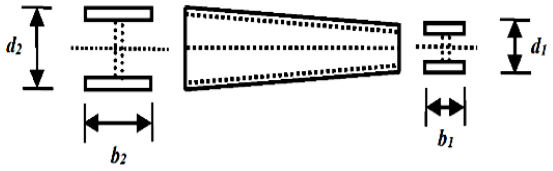

(a) Varying both of depth, d and width, b (n=3)

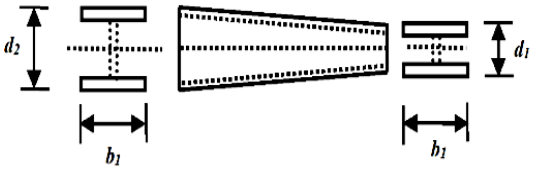

(b) Varying depth, d and constant width, b (n=2)

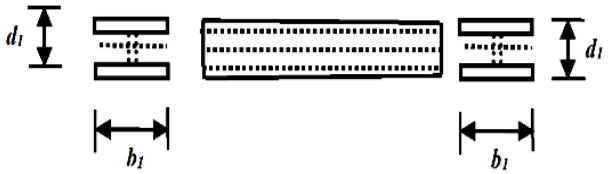

(c) Constant both of depth d and width, b (n=0)

Fig. 2 Various cross-sectional shape factors for linear tapered I-section member

length of I-section web-tapered members is approximated as parabolic function (i.e., n=2). It should be mentioned that when the member is uniform, n equals to zero (Fig. 2(c)).

Based on the Euler-Bernoulli beam-column theory, the governing fourth-order differential equations for the columns and beams are written as below:

$$\left.\begin{aligned}
&\frac{d^2}{dx_1^2}\left[EI_c\left(\frac{x_1}{a}\right)^n\frac{d^2w_1}{dx_1^2}\right]+P_1\frac{d^2w_1}{dx_1^2}=0\\
&\frac{d^2}{dx_2^2}\left[EI_b\left(\frac{x_2}{b}\right)^n\frac{d^2w_2}{dx_2^2}\right]=0\\
&\frac{d^2}{dx_3^2}\left[EI_b\left(\frac{x_3}{b}\right)^n\frac{d^2w_3}{dx_3^2}\right]=0\\
&\frac{d^2}{dx_4^2}\left[EI_c\left(\frac{x_4}{a}\right)^n\frac{d^2w_4}{dx_4^2}\right]+P_4\frac{d^2w_4}{dx_4^2}=0
\end{aligned}\right\} \tag{2}$$

For the shape factors n=0, 2 and 3, the general solutions of Eq. (2), are presented in Eqs. (3)-(5), respectively.

$$\left.\begin{aligned}
w_1&=A_1\sin\left(\frac{\rho x_1}{l_c}\right)+B_1\cos\left(\frac{\rho x_1}{l_c}\right)+C_1x_1+D_1\\
w_2&=A_2x_2^3+B_2x_2^2+C_2x_2+D_2\\
w_3&=A_3x_3^3+B_3x_3^2+C_3x_3+D_3\\
w_4&=A_4\sin\left(\frac{\rho x_4}{l_c}\right)+B_4\cos\left(\frac{\rho x_4}{l_c}\right)+C_4x_4+D_4
\end{aligned}\right\} \tag{3}$$

$$\left.\begin{aligned}
w_1 &= \sqrt{\frac{x_1}{a}}\left\{A_1 \sin\left[\sqrt{\left(\frac{\bar{a}\rho}{1-\bar{a}}\right)^2-\frac{1}{4}}\times ln\left(\frac{x_1}{a}\right)\right]+B_1\cos\left[\sqrt{\left(\frac{\bar{a}\rho}{1-\bar{a}}\right)^2-\frac{1}{4}}\times ln\left(\frac{x_1}{a}\right)\right]\right\}+C_1x_1+D_1\\
w_2 &= A_2x_2+B_2xLn\left(\frac{x_2}{h}\right)+C_2+D_2Ln\left(\frac{x_2}{h}\right)\\
w_3 &= A_3x_3+B_3xLn\left(\frac{x_3}{h}\right)+C_3+D_3Ln\left(\frac{x_3}{h}\right)\\
w_4 &= \sqrt{\frac{x_4}{a}}\left\{A_4 \sin\left[\sqrt{\left(\frac{\bar{a}\rho}{1-\bar{a}}\right)^2-\frac{1}{4}}\times ln\left(\frac{x_4}{a}\right)\right]+B_4\cos\left[\sqrt{\left(\frac{\bar{a}\rho}{1-\bar{a}}\right)^2-\frac{1}{4}}\times ln\left(\frac{x_4}{a}\right)\right]\right\}+C_4x_4+D_4
\end{aligned}\right\} \quad (4)$$

$$\left.\begin{aligned}
w_1 &= \sqrt{x_1}\left[A_1 BesselY\left(\frac{2\bar{a}\rho}{1-\bar{a}}\sqrt{\frac{a}{x_1}}\right)+B_1 BesselJ\left(\frac{2\bar{a}\rho}{1-\bar{a}}\sqrt{\frac{a}{x_1}}\right)\right]+C_1x_1+D_1\\
w_2 &= A_2+B_2\ln\left(\frac{x_2}{h}\right)+C_2x_2+\frac{D_2}{x_2}\\
w_3 &= A_3+B_3\ln\left(\frac{x_3}{h}\right)+C_3x_3+\frac{D_3}{x_3}\\
w_4 &= \sqrt{x_4}\left[A_4 BesselY\left(\frac{2\bar{a}\rho}{1-\bar{a}}\sqrt{\frac{a}{x_4}}\right)+B_4 BesselJ\left(\frac{2\bar{a}\rho}{1-\bar{a}}\sqrt{\frac{a}{x_4}}\right)\right]+C_4x_4+D_4
\end{aligned}\right\} \quad (5)$$

where $\rho^2 = Pl_c^2/EI_c$, $\bar{a} = a/(a+l_c) = a/h$ and A_i, B_i, C_i, and D_i (i=1,2,3,4) are integration constants to be determined using boundary and kinematic conditions. These constants can be obtained from Tables 1 and 2, for prismatic and non-prismatic gabled frame, respectively. It should be mentioned that the bending moments have the following formula:

$$M_i(x_i) = -EI_i(x_i)\frac{d^2w_i}{dx_i^2} \qquad (i=1,4) \quad (6)$$

On the other hand, the shear forces of the columns have the following form:

$$V_i(x_i) = -\frac{d}{dx_i}\left(EI_i(x_i)\frac{d^2w_i}{dx_i^2}\right)-P_i\frac{dw_i}{dx_i} \qquad (i=1,4) \quad (7)$$

The corresponding bending moment and shear force of the beams can be determined from the following equations:

$$M_j(x_j) = -EI_j(x_j)\frac{d^2w_j}{dx_j^2} \qquad (j=2,3) \quad (8)$$

$$V_j(x_j) = -\frac{d}{dx_i}\left(EI_j(x_j)\frac{d^2w_j}{dx_j^2}\right) \qquad (j=2,3) \quad (9)$$

In practice, both columns and beams in a gabled frame have the same sectional properties (i.e.,

Table 1 Kinematic and boundary conditions of a uniform gabled frame (i.e., Fig. 1(a))

Joint	Condition
1	$w_1(0)=0$ $M_1(0)+K_{fL}w'_1(0)=0$
2	$w_2(l_b)-w_1(l_c)\sin\alpha=0$ $w_1(l_c)-w_4(l_c)=0$ $M_1(l_c)+M_2(l_b)=0$ $M_2(l_b)=K_{cL}[w'_2(l_b)-w'_1(l_c)]$
3	$w_2(0)-w_1(l_c)\sin\alpha=0$ $w_3(0)-w_4(l_c)\sin\alpha=0$ $M_2(0)+M_3(0)=0$ $w'_2(0)-w'_3(0)=0$
4	$w_3(l_c)-w_4(l_c)\sin\alpha=0$ $V_1(l_c)+V_4(l_c)+K_bw_4(l_c)=0$ $M_2(l_b)+M_4(l_c)=0$ $M_3(l_b)=K_{cR}[w'_3(l_b)-w'_4(l_c)]$
5	$w_4(0)=0$ $M_4(0)+K_{fR}w'_4(0)=0$

Table 2 Kinematic and boundary conditions of a non-uniform gabled frame (i.e., Fig. 1(b))

Joint	Condition
1	$w_1(a)=0$ $M_1(a)+K_{fL}w'_1(a)=0$
2	$w_2(g)-w_1(h)\sin\alpha=0$ $w_1(h)-w_4(h)=0$ $M_1(h)+M_2(g)=0$ $M_2(g)=K_{cL}[w'_2(g)-w'_1(h)]$
3	$w_2(b)-w_1(h)\sin\alpha=0$ $w_3(b)-w_4(h)\sin\alpha=0$ $M_2(b)+M_3(b)=0$ $w'_2(b)-w'_3(b)=0$
4	$w_3(g)-w_4(h)\sin\alpha=0$ $V_1(h)+V_4(h)+K_bw_4(h)=0$ $M_3(g)+M_4(h)=0$ $M_3(g)=K_{cR}[w'_3(g)-w'_4(h)]$
5	$w_4(a)=0$ $M_4(a)+K_{fR}w'_4(a)=0$

$I_1(x_1)=I_4(x_4)$ and $I_2(x_2)=I_3(x_3)$), and mostly loaded by equal loads (i.e. $P_1 = P_4$). Accordingly, it is assumed that $P_1=P_4=P$, $I_1=I_4$ and $I_2=I_3$. At this stage, a gabled frame with tapered members, as shown in Fig. 1(b), will be analyzed. By utilizing the boundary and kinematic conditions, and also the following dimensionless parameters, $\rho^2 = Pl_c^2/EI_c$, $\overline{\mu} = I_b/I_c$, $\overline{l} = l_b/l_c$, $\overline{a} = a/h$, $\overline{b} = b/h$, $\overline{g} = g/h$, $\overline{K}_{cR} = 1/(1+EI_b/K_{cR}l_b)$, $\overline{K}_{fL} = 1/(1+EI_c/K_{fL}l_c)$,

$\overline{K}_{fR}=1/(1+EI_c/K_{fR}l_c)$, $\overline{K}_b=1/(1+EI_c/K_b l_c^3)$ the following system of non-dimensional equations for shape factor n=3, can be written as:

$$
\left.\begin{aligned}
&\overline{A}_1 Y_{\bar{a},1}+\overline{B}_1 J_{\bar{a},1}+\overline{C}_1+\overline{D}_1=0\\
&\overline{K}_{fL}\left\{\overline{A}_1\left[Y_{\bar{a},1}\left(1-\bar{a}-\bar{a}\rho^2\right)+Y_{\bar{a},0}\left(-\bar{a}\rho\right)\right]+\overline{B}_1\left[J_{\bar{a},1}\left(1-\bar{a}-\bar{a}\rho^2\right)+J_{\bar{a},0}\left(-\bar{a}\rho\right)\right]+\right.\\
&\left.\overline{C}_1(1-\bar{a})\right\}+\bar{a}\rho\left(\overline{A}_1 Y_{\bar{a},1}+\overline{B}_1 J_{\bar{a},1}\right)=0\\
&\overline{A}_4 Y_{\bar{a},1}+\overline{B}_4 J_{\bar{a},1}+\overline{C}_4+\overline{D}_4=0\\
&\overline{K}_{fR}\left\{\overline{A}_4\left[Y_{\bar{a},1}\left(1-\bar{a}-\bar{a}\rho^2\right)+Y_{\bar{a},0}\left(-\bar{a}\rho\right)\right]+\overline{B}_4\left[J_{\bar{a},1}\left(1-\bar{a}-\bar{a}\rho^2\right)+J_{\bar{a},0}\left(-\bar{a}\rho\right)\right]+\right.\\
&\left.\overline{C}_4(1-\bar{a})\right\}+\bar{a}\rho\left(\overline{A}_4 Y_{\bar{a},1}+\overline{B}_4 J_{\bar{a},1}\right)=0\\
&\left(\overline{A}_1 Y_1+\overline{B}_1 J_1+\frac{\overline{C}_1}{\sqrt{\bar{a}}}+\overline{D}_1\sqrt{\bar{a}}\right)\left(-\sin\alpha\right)+\overline{A}_2+\overline{B}_2\ln\bar{b}+\overline{C}_2\bar{b}+\frac{\overline{D}_2}{\bar{b}}=0\\
&\left(\overline{A}_1 Y_1+\overline{B}_1 J_1+\frac{\overline{C}_1}{\sqrt{\bar{a}}}+\overline{D}_1\sqrt{\bar{a}}\right)\left(-\sin\alpha\right)+\overline{A}_2+\overline{B}_2\ln\bar{g}+\overline{C}_2\bar{g}+\frac{\overline{D}_2}{\bar{g}}=0\\
&\left(\overline{A}_4 Y_1+\overline{B}_4 J_1+\frac{\overline{C}_4}{\sqrt{\bar{a}}}+\overline{D}_4\sqrt{\bar{a}}\right)\left(-\sin\alpha\right)+\overline{A}_3+\overline{B}_3\ln\bar{b}+\overline{C}_3\bar{b}+\frac{\overline{D}_3}{\bar{b}}=0\\
&\left(\overline{A}_4 Y_1+\overline{B}_4 J_1+\frac{\overline{C}_4}{\sqrt{\bar{a}}}+\overline{D}_4\sqrt{\bar{a}}\right)\left(-\sin\alpha\right)+\overline{A}_3+\overline{B}_3\ln\bar{g}+\overline{C}_3\bar{g}+\frac{\overline{D}_3}{\bar{g}}=0\\
&Y_1(\overline{A}_1-\overline{A}_4)+J_1(\overline{B}_1-\overline{B}_4)+\frac{\overline{C}_1-\overline{C}_4}{\sqrt{\bar{a}}}+\left(\overline{D}_1-\overline{D}_4\right)\sqrt{\bar{a}}=0\\
&\overline{K}_b\left[\rho^2(1-\bar{a})(\overline{C}_1+\overline{C}_4)+\overline{A}_4\sqrt{\bar{a}}Y_1+\overline{B}_4\sqrt{\bar{a}}J_1+\overline{C}_4+\overline{D}_4\bar{a}\right]-\rho^2(1-\bar{a})(\overline{C}_1+\overline{C}_4)=0\\
&\rho^2\left(\overline{A}_1 Y_1+\overline{B}_1 J_1\right)+\overline{\mu}\frac{(1-\bar{a})^2}{\bar{b}^3}\left(\overline{B}_2\bar{g}-2\overline{D}_2\right)=0\\
&\overline{K}_{cL}\left\{\overline{A}_1\left[-Y_1+Y_0\left(\frac{\bar{a}^{\frac{3}{2}}\rho}{1-\bar{a}}\right)\right]+\overline{B}_1\left[-J_1+J_0\left(\frac{\bar{a}^{\frac{3}{2}}\rho}{1-\bar{a}}\right)\right]\right.\\
&\left.-\frac{\overline{C}_1}{\sqrt{\bar{a}}}+\frac{\overline{B}_2}{\bar{g}}+\overline{C}_2-\frac{\overline{D}_2}{\bar{g}^2}+\frac{1}{\bar{b}^2}\left(1-\frac{\bar{g}}{\bar{b}}\right)\left(2\overline{D}_2-\overline{B}_2\bar{g}\right)\right\}+\frac{1}{\bar{b}^2}\left(1-\frac{\bar{g}}{\bar{b}}\right)\left(\overline{B}_2\bar{g}-2\overline{D}_2\right)=0\\
&\rho^2\left(\overline{A}_4 Y_1+\overline{B}_4 J_1\right)+\overline{\mu}\frac{(1-\bar{a})^2}{\bar{b}^3}\left(\overline{B}_3\bar{g}-2\overline{D}_3\right)=0\\
&\overline{K}_{cR}\left\{\overline{A}_4\left[-Y_1+Y_0\left(\frac{\bar{a}^{\frac{3}{2}}\rho}{1-\bar{a}}\right)\right]+\overline{B}_4\left[-J_1+J_0\left(\frac{\bar{a}^{\frac{3}{2}}\rho}{1-\bar{a}}\right)\right]\right.\\
&\left.-\frac{\overline{C}_4}{\sqrt{\bar{a}}}+\frac{\overline{B}_3}{\bar{g}}+\overline{C}_3-\frac{\overline{D}_3}{\bar{g}^2}+\frac{1}{\bar{b}^2}\left(1-\frac{\bar{g}}{\bar{b}}\right)\left(2\overline{D}_3-\overline{B}_3\bar{g}\right)\right\}+\frac{1}{\bar{b}^2}\left(1-\frac{\bar{g}}{\bar{b}}\right)\left(\overline{B}_3\bar{g}-2\overline{D}_3\right)=0\\
&\frac{\overline{B}_2}{\bar{b}}-\frac{2\overline{D}_2}{\bar{b}^2}+\frac{\overline{B}_3}{\bar{b}}-\frac{2\overline{D}_3}{\bar{b}^2}=0\\
&\frac{\left(\overline{B}_2-\overline{B}_3\right)}{\bar{b}}+\left(\overline{C}_2-\overline{C}_3\right)+\frac{\left(\overline{D}_3-\overline{D}_2\right)}{\bar{b}^2}=0
\end{aligned}\right\}
\tag{10}
$$

The non-dimensional constants $\overline{A}_1 = A_1$, $\overline{B}_1 = B_1$, $\overline{C}_1 = C_1\sqrt{a}$, $\overline{D}_1 = D_1/\sqrt{a}$, $\overline{A}_2 = A_2/\sqrt{h}$, $\overline{B}_2 = B_2/\sqrt{h}$, $\overline{C}_2 = C_2\sqrt{h}$, $\overline{D}_2 = D_2/\sqrt{h^3}$, $\overline{A}_3 = A_3/\sqrt{h}$, $\overline{B}_3 = B_3/\sqrt{h}$, $\overline{C}_3 = C_3\sqrt{h}$, $\overline{D}_3 = D_3/\sqrt{h^3}$, $\overline{A}_4 = A_4$, $\overline{B}_4 = B_4$, $\overline{C}_4 = C_4\sqrt{a}$, $\overline{D}_4 = D_4/\sqrt{a}$ are utilized. The following abbreviations can be used for simplifications:

$$Y_{\bar{a},1} = BesselY\left(1, \frac{2\bar{a}\rho}{1-\bar{a}}\right),\quad J_{\bar{a},1} = BesselJ\left(1, \frac{2\bar{a}\rho}{1-\bar{a}}\right),\quad Y_{\bar{a},0} = BesselY\left(0, \frac{2\bar{a}\rho}{1-\bar{a}}\right),\quad J_{\bar{a},0} = BesselJ\left(0, \frac{2\bar{a}\rho}{1-\bar{a}}\right),$$

$$Y_1 = BesselY\left(1, \frac{2\bar{a}^{\frac{3}{2}}\rho}{1-\bar{a}}\right),\quad J_1 = BesselJ\left(1, \frac{2\bar{a}^{\frac{3}{2}}\rho}{1-\bar{a}}\right),\quad Y_0 = BesselY\left(0, \frac{2\bar{a}^{\frac{3}{2}}\rho}{1-\bar{a}}\right),\quad J_0 = BesselJ\left(0, \frac{2\bar{a}^{\frac{3}{2}}\rho}{1-\bar{a}}\right).$$

When the shape factor n is equal to 2, the following system of dimensionless equations can be similarly obtained:

$$\left.\begin{aligned}
&\overline{B}_1\sqrt{\bar{a}} + \overline{C}_1\bar{a} + \overline{D}_1 = 0\\
&\overline{K}_{fL}\sqrt{\bar{a}}\left\{(1-\bar{a})\left[\overline{A}_1\left(\sqrt{\left(\frac{\bar{a}\rho}{1-\bar{a}}\right)^2 - \frac{1}{4}}\right) + \overline{B}_1/2 + \overline{C}_1\sqrt{\bar{a}}\right] - \overline{B}_1\bar{a}\rho^2\right\} + \overline{B}_1\bar{a}\sqrt{\bar{a}}\rho^2 = 0\\
&\overline{B}_4\sqrt{\bar{a}} + \overline{C}_4\bar{a} + \overline{D}_4 = 0\\
&\overline{K}_{fR}\sqrt{\bar{a}}\left\{(1-\bar{a})\left[\overline{A}_4\left(\sqrt{\left(\frac{\bar{a}\rho}{1-\bar{a}}\right)^2 - \frac{1}{4}}\right) + \overline{B}_4/2 + \overline{C}_4\sqrt{\bar{a}}\right] - \overline{B}_4\bar{a}\rho^2\right\} + \overline{B}_4\bar{a}\sqrt{\bar{a}}\rho^2 = 0\\
&\left(\overline{A}_1\sin\beta + \overline{B}_1\cos\beta + \overline{C}_1 + \overline{D}_1\right)(-\sin\alpha) + \bar{b}\left(\overline{A}_2 + \overline{B}_2\ln\bar{b}\right) + \overline{C}_2 + \overline{D}_2\ln\bar{b} = 0\\
&\left(\overline{A}_1\sin\beta + \overline{B}_1\cos\beta + \overline{C}_1 + \overline{D}_1\right)(-\sin\alpha) + \bar{g}\left(\overline{A}_2 + \overline{B}_2\ln\bar{g}\right) + \overline{C}_2 + \overline{D}_2\ln\bar{g} = 0\\
&\left(\overline{A}_4\sin\beta + \overline{B}_4\cos\beta + \overline{C}_4 + \overline{D}_4\right)(-\sin\alpha) + \bar{b}\left(\overline{A}_3 + \overline{B}_3\ln\bar{b}\right) + \overline{C}_3 + \overline{D}_3\ln\bar{b} = 0\\
&\left(\overline{A}_4\sin\beta + \overline{B}_4\cos\beta + \overline{C}_4 + \overline{D}_4\right)(-\sin\alpha) + \bar{g}\left(\overline{A}_3 + \overline{B}_3\ln\bar{g}\right) + \overline{C}_3 + \overline{D}_3\ln\bar{g} = 0\\
&\sin\beta(\overline{A}_1 - \overline{A}_4) + \cos\beta(\overline{B}_1 - \overline{B}_4) + \overline{C}_1 - \overline{C}_4 + \overline{D}_1 - \overline{D}_4 = 0\\
&\overline{K}_b\left[\rho^2(1-\bar{a})(\overline{C}_1 + \overline{C}_4) + \overline{A}_4\sin\beta + \overline{B}_4\cos\beta + \overline{C}_4 + \overline{D}_4\right] - \rho^2(1-\bar{a})(\overline{C}_1 + \overline{C}_4) = 0\\
&\rho^2\left(\overline{A}_1\sin\beta + \overline{B}_1\cos\beta\right) + \bar{\mu}\frac{(1-\bar{a})^2}{\bar{b}^2}\left(\overline{D}_2 - \overline{B}_2\bar{g}\right) = 0\\
&\overline{K}_{cL}\left\{\sin\beta\left[\left(\sqrt{\left(\frac{\bar{a}\rho}{1-\bar{a}}\right)^2 - \frac{1}{4}}\right)\overline{B}_1 - \overline{A}_1/2\right] - \cos\beta\left[\left(\sqrt{\left(\frac{\bar{a}\rho}{1-\bar{a}}\right)^2 - \frac{1}{4}}\right)\overline{A}_1 - \overline{B}_1/2\right] + \right.\\
&\left.\overline{A}_2 - \overline{C}_1 + \overline{B}_2\left(1 + \ln\bar{g}\right) + \frac{\overline{D}_2}{\bar{g}} + \frac{1}{\bar{b}}\left(1 - \frac{\bar{g}}{\bar{b}}\right)\left(\overline{B}_2\bar{g} - \overline{D}_2\right)\right\} + \frac{1}{\bar{b}}\left(1 - \frac{\bar{g}}{\bar{b}}\right)\left(\overline{D}_2 - \overline{B}_2\bar{g}\right) = 0\\
&\rho^2\left(\overline{A}_4\sin\beta + \overline{B}_4\cos\beta\right) + \bar{\mu}\frac{(1-\bar{a})^2}{\bar{b}^2}\left(\overline{D}_3 - \overline{B}_3\bar{g}\right) = 0
\end{aligned}\right\}$$

$$
\left.\begin{array}{l}
\overline{K}_{cR}\left\{\sin\beta\left[\left(\sqrt{\left(\dfrac{\overline{a}\rho}{1-\overline{a}}\right)^2-\dfrac{1}{4}}\right)\overline{B}_4-\overline{A}_4/2\right]-\cos\beta\left[\left(\sqrt{\left(\dfrac{\overline{a}\rho}{1-\overline{a}}\right)^2-\dfrac{1}{4}}\right)\overline{A}_4-\overline{B}_4/2\right]+\right. \\
\left.\overline{A}_3-\overline{C}_4+\overline{B}_3\left(1+\ln\overline{g}\right)+\dfrac{\overline{D}_3}{\overline{g}}+\dfrac{1}{\overline{b}}\left(1-\dfrac{\overline{g}}{\overline{b}}\right)\left(\overline{B}_3\overline{g}-\overline{D}_3\right)\right\}+\dfrac{1}{\overline{b}}\left(1-\dfrac{\overline{g}}{\overline{b}}\right)\left(\overline{D}_3-\overline{B}_3\overline{g}\right)=0 \\
-\overline{B}_2+\dfrac{\overline{D}_2}{\overline{b}}-\overline{B}_3+\dfrac{\overline{D}_3}{\overline{b}}=0 \\
\overline{A}_2-\overline{A}_3+\left(1+\ln\overline{b}\right)\left(\overline{B}_2-\overline{B}_3\right)+\dfrac{\left(\overline{D}_2-\overline{D}_3\right)}{\overline{b}}=0
\end{array}\right. \tag{11}
$$

In the above relationships, the subsequent dimensionless constants are assumed:

$$
\overline{A}_1=A_1/\sqrt{a},\ \overline{B}_1=B_1/\sqrt{a},\ \overline{C}_1=C_1h,\ \overline{D}_1=D_1,\ \overline{A}_2=A_2h,\ \overline{B}_2=B_2h,\ \overline{C}_2=C_2,\ \overline{D}_2=D_2,
$$

$$
\overline{A}_3=A_3h,\ \overline{B}_3=B_3h,\ \overline{C}_3=C_3,\ \overline{D}_3=D_3,\ \overline{A}_4=A_4/\sqrt{a},\ \overline{B}_4=B_4/\sqrt{a},\ \overline{C}_4=C_4h,\ \overline{D}_4=D_4,
$$

$$
\beta=\sqrt{\left(\frac{\overline{a}\rho}{1-\overline{a}}\right)^2-\frac{1}{4}}\times\ln\left(\frac{1}{\overline{a}}\right).
$$

For the gabled frame with uniform members, the following system of non-dimensional equations can be derived:

$$
\left.\begin{array}{l}
\overline{B}_1+\overline{D}_1=0 \\
\overline{K}_{fL}\left[\rho\left(\overline{A}_1-\overline{B}_1\rho\right)+\overline{C}_1\right]+\overline{B}_1\rho^2=0 \\
\overline{B}_4+\overline{D}_4=0 \\
\overline{K}_{fR}\left[\rho\left(\overline{A}_4-\overline{B}_4\rho\right)+\overline{C}_4\right]+\overline{B}_4\rho^2=0 \\
\left(\overline{A}_1\sin\rho+\overline{B}_1\cos\rho+\overline{C}_1+\overline{D}_1\right)\left(-\sin\alpha\right)+\overline{D}_2\bar{l}=0 \\
\left(\overline{A}_1\sin\rho+\overline{B}_1\cos\rho+\overline{C}_1+\overline{D}_1\right)\left(-\sin\alpha\right)+\bar{l}\left[\bar{l}\left(\overline{A}_2\bar{l}+\overline{B}_2\right)+\overline{C}_2+\overline{D}_2\right]=0 \\
\left(\overline{A}_4\sin\rho+\overline{B}_4\cos\rho+\overline{C}_4+\overline{D}_4\right)\left(-\sin\alpha\right)+\overline{D}_3\bar{l}=0 \\
\left(\overline{A}_4\sin\rho+\overline{B}_4\cos\rho+\overline{C}_4+\overline{D}_4\right)\left(-\sin\alpha\right)+\bar{l}\left[\bar{l}\left(\overline{A}_3\bar{l}+\overline{B}_3\right)+\overline{C}_3+\overline{D}_3\right]=0 \\
\left(\overline{A}_1-\overline{A}_4\right)\sin\rho+\left(\overline{B}_1-\overline{B}_4\right)\cos\rho+\overline{C}_1-\overline{C}_4+\overline{D}_1-\overline{D}_4=0 \\
\overline{K}_b\left[\rho^2\left(\overline{C}_1+\overline{C}_4\right)+\overline{C}_4+\overline{D}_4+\overline{A}_4\sin\rho+\overline{B}_4\cos\rho\right]-\rho^2\left(\overline{C}_1+\overline{C}_4\right)=0 \\
\rho^2\left(\overline{A}_1\sin\rho+\overline{B}_1\cos\rho\right)-2\overline{\mu}\left(3\overline{A}_2\bar{l}+\overline{B}_2\right)=0 \\
\overline{K}_{cL}\left[\rho\left(\overline{B}_1\sin\rho-\overline{A}_1\cos\rho\right)-3\overline{A}_2\left(\bar{l}\right)^2+\overline{C}_2-\overline{C}_1\right]+2\bar{l}\left(3\overline{A}_2\bar{l}+\overline{B}_2\right)=0 \\
\rho^2\left(\overline{A}_4\sin\rho+\overline{B}_4\cos\rho\right)-2\overline{\mu}\left(3\overline{A}_3\bar{l}+\overline{B}_3\right)=0 \\
\overline{K}_{cR}\left[\rho\left(\overline{B}_4\sin\rho-\overline{A}_4\cos\rho\right)-3\overline{A}_3\left(\bar{l}\right)^2+\overline{C}_3-\overline{C}_4\right]+2\bar{l}\left(3\overline{A}_3\bar{l}+\overline{B}_3\right)=0 \\
-\left(\overline{B}_2+\overline{B}_3\right)=0 \\
\overline{C}_2-\overline{C}_3=0
\end{array}\right\} \tag{12}
$$

in which, $\overline{A}_1 = A_1 / l_c$, $\overline{B}_1 = B_1 / l_c$, $\overline{C}_1 = C_1$, $\overline{D}_1 = D_1 / l_c$, $\overline{A}_2 = A_2 l_c^2$, $\overline{B}_2 = B_2 l_c$, $\overline{C}_2 = C_2$, $\overline{D}_2 = D_2 / l_b$, $\overline{A}_3 = A_3 l_c^2$, $\overline{B}_3 = B_3 l_c$, $\overline{C}_3 = C_3$, $\overline{D}_3 = D_3 / l_b$, $\overline{A}_4 = A_4 / l_c$, $\overline{B}_4 = B_4 / l_c$, $\overline{C}_4 = C_4$, $\overline{D}_4 = D_4 / l_c$.

At this stage, the determinant of Eqs. (10)-(12) is set to zero. This leads to the non-dimensional critical load factor, ρ^2_{cr}, of the uniform (i.e., n=0) and non-uniform (i.e., n=2 and n=3) gabled frames, with flexible connections and elastic supports.

$$\det \mathbf{K}=0 \tag{13}$$

The matrix **K**, which includes parameters for the various shape factors (i.e., n=0, 2 and 3) are explicitly given in the Appendix A. By solving Eq. (13), the dimensionless critical load factor, ρ^2_{cr}, can be found. Consequently, the following frame buckling load will be obtained:

$$P_{cr} = \rho^2_{cr} \frac{EI_c}{l_c^2} = \overline{\rho}^2_{cr} \frac{EI_m}{l_c^2} = \frac{\pi^2 EI_m}{(Kl_c)^2} \tag{14}$$

As a result, the equivalent effective length factor of column, K, is computed in the following form:

$$K = \frac{\pi}{\sqrt{\overline{\rho}^2_{cr}}} \tag{15}$$

It should be noted that $\overline{\rho}^2_{cr} = P_{cr} l_c^2 / EI_m$ is the dimensionless equivalent critical load factor and represents the load-carrying capacity of the frame. Moreover, I_m is the moment of inertia at the middle of the column (i.e., for $x=a+0.5l_c$). For uniform column, $I_m = I_c$.

3. Verification and numerical examples

In order to demonstrate the efficiency, accuracy and application of the suggested method, four numerical examples are analyzed in this section. The findings are compared with those obtained by other methods.

3.1 Example 1

As shown in Fig. 3, critical load of the gabled frame, with tapered web I-section members is given by the dimensionless design charts (AISC 1999, Saffari *et al*. 2008). Steel I-section tapered columns have total depth varying linearly from a depth of 21 cm at supports 1 and 5 to a depth of 61 cm at eave points. Furthermore, for the steel beams, the total depth varies linearly from 61 cm at the eave points to a depth of 37 cm at the apex point. Accordingly, the members' moments of inertia at the foundations (I_c), eaves ($I_{c\text{-}b}=I_{b\text{-}c}$) and apex ($I_b$) are 1527 cm^4, 18181 cm^4 and 5552 cm^4, respectively. The materials' elastic modulus is 2.1×10^6 kg/cm^2. It should be noted that the moment of inertia variations for all structural members is parabolic (i.e., n=2).

The required parameters for stability matrix, as given in Appendix A, are calculated as follows:

$$\overline{a} = \frac{a}{h} = \frac{244.84}{244.84+600} = 0.2898,\quad \overline{b} = \frac{b}{h} = \frac{827.56}{244.84+600} = 0.9795,\quad \overline{g} = \frac{g}{h} = \frac{827.56+670}{244.84+600} = 1.7726$$

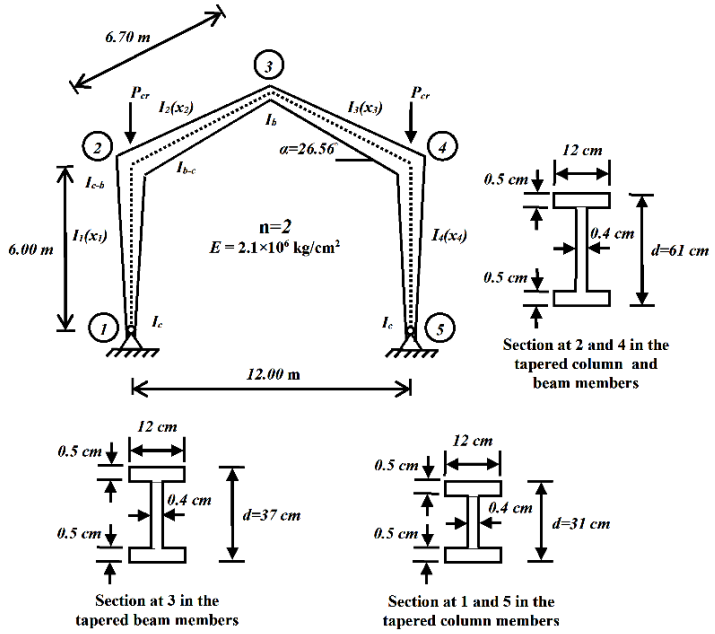

Fig. 3 Geometry and material constants of steel gabled frame with tapered I-section members and hinged supports (example 1)

Table 3 Comparison of the critical loads, P_{cr}(kN), of the gabled frame in example 1

Proposed method	Saffari *et al*. (2008)	AISC (1999)	F.E.M. (100elements)
89	85	88	89

$$\alpha = 26.56^{\circ},\ \ \overline{\mu} = \frac{5552}{1527} = 3.6359,\ \ \overline{K}_{fL} = \overline{K}_{fR} = 0.0,\ \ \overline{K}_{cL} = \overline{K}_{cR} = 1.0,\ \ \overline{K}_{b} = 0.0\,.$$

Using non-dimensional factors obtained above and solving Eq. (13) for n=2, the buckling load of the frame is given by Eq. (14). Comparisons of the result with the other methods are presented in Table 3. By dividing each member into 100 elements (for finding exact response), the exact buckling load was checked using finite element program belong to Ferdowsi University of Mashhad. Based on the obtained results, it is observed that the proposed method for calculating the critical load has a high accuracy.

3.2 Example 2

Saffari *et al*. (2008) studied the steel gabled frame with tapered members shown in Fig. 4. By extended slope-deflection relations, the effective length factor of the frame was obtained for the two cases of hinged and fixed supports. The columns' moments of inertia at the eaves ($I_{c\text{-}b}$) and bases (I_c) are 50000 cm^4 and 5000 cm^4, respectively. The modulus of elasticity is 2.1×10^6 kg/cm^2. The beams' moments of inertia at the eaves ($I_{b\text{-}c}$) and apex (I_b) are 30000 cm^4 and 4000 cm^4, respectively. The critical load and equivalent effective length factor can be obtained from Eqs. (14) and (15), respectively. A value of n=2 and the following non-dimensional parameters are used:

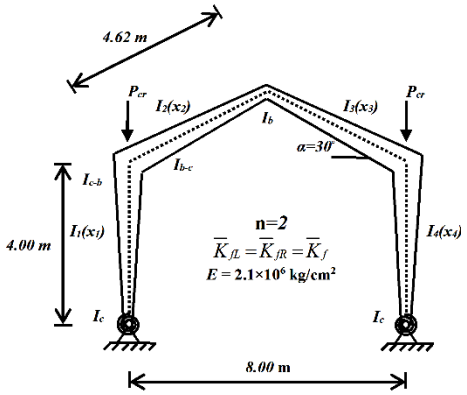

Fig. 4 Geometry and material constants of steel gabled frame with tapered I-section members and various bases (example 2)

Table 4 Comparison of the effective length factor, *K*, of the gabled frame in example 2

Type of foundations	Proposed method	Saffari *et al*. (2008)	F.E.M. (100elements)
Hinged ($\overline{K}_f=0.0$)	2.611	2.610	2.611
Semi-Rigid ($\overline{K}_f=0.5$)	2.341	-	2.341
Fixed ($\overline{K}_f=1.0$)	1.619	1.619	1.619

$$\overline{a}=\frac{a}{h}=\frac{184.99}{184.99+400}=0.3162,\ \overline{b}=\frac{b}{h}=\frac{265.66}{184.99+400}=0.4541,\ \overline{g}=\frac{g}{h}=\frac{265.66+461.88}{184.99+400}=1.2437,$$

$$\alpha=30^\circ,\ \overline{\mu}=\frac{4000}{5000}=0.8,\ \overline{K}_{fL}=\overline{K}_{fR}=\overline{K}_f=0.0-0.50-1.0,\ \overline{K}_{cL}=\overline{K}_{cR}=1.0,\ \overline{K}_b=0.0.$$

Table 4 demonstrates the results of present study, as well as those of other approaches. According to the results, the predictions of the proposed technique agree well with those of other methods.

3.3 Example 3

As shown in Fig. 5, the unbraced steel gabled frame composed of tapered I-section members is considered. This frame was analyzed by Safavi and Moharami (2009). According to Fig. 5, the members' moments of inertia at the points 1, 2 and 3 are I_c=3691 cm^4, $I_{c\text{-}b}$=$I_{b\text{-}c}$=18181 cm^4 and I_b=5552 cm^4, respectively. The material modulus of elasticity is 2.1×10^6 kg/cm^2. The required dimensionless factors for the stability matrix, **K**, are computed as follows:

$$\overline{a}=\frac{a}{h}=\frac{492.04}{492.04+600}=0.4506,\ \overline{b}=\frac{b}{h}=\frac{827.56}{492.04+600}=0.7578,\ \overline{g}=\frac{g}{h}=\frac{827.56+670}{492.04+600}=1.3713,\ \alpha=26.56^\circ,$$

$$\overline{\mu}=\frac{5552}{3691}=1.5042,\ \overline{K}_{fL}=\overline{K}_{fR}=0.0,\ \overline{K}_{cL}=\overline{K}_{cR}=1.0,\ \overline{K}_b=0.0.$$

Using n=2 and the foregoing parameters Eq. (13) can be solved for the non-dimensional critical load factor ρ^2_{cr}. The buckling load can then be calculated form Eq. (14). The results are presented

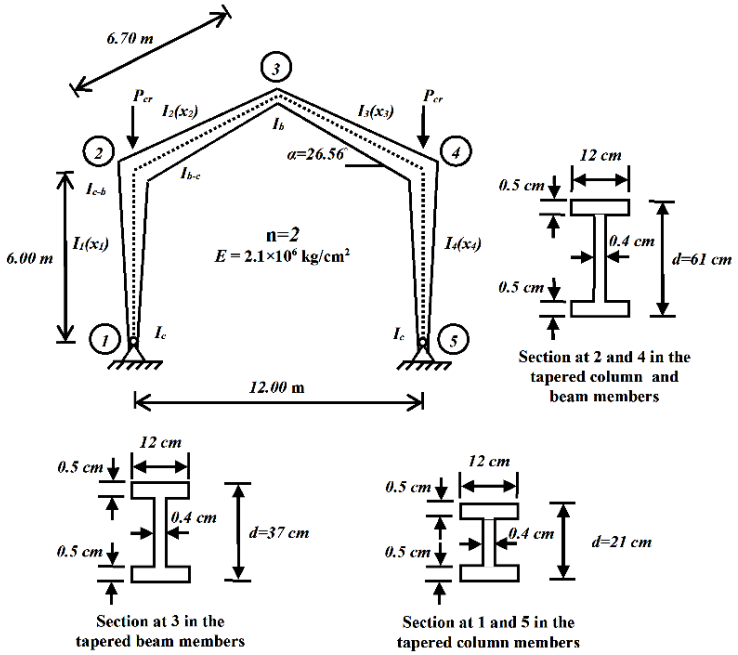

Fig. 5 Geometry and material constants of steel gabled frame with tapered I-section members and hinged supports (example 3)

Table 5 Comparison of the buckling loads, P_{cr} (kN), of the gabled frame in example 3

Proposed method	Safavi and Moharami (2009)	AISC (1999)	F.E.M. (100elements)
100	97	98	99

in Table 5. It is reminded that the solution of Safavi and Moharami (2009) is based on equating the external work on the frame to its internal flexural strain energy of buckling. From Table 5, it is observed that the results of the proposed method are very close to the values obtained by other methods.

3.4 Example 4

In this example, the stability of steel gabled frame with different shape factors and various supports, as shown in Fig. 6, will be investigated. Recently, Tajmir Riahi *et al*. (2012) studied the stability of this frame for shape factor n=2, using the slope-deflection method. The modulus of elasticity is 2.0×10^8 kN/m^2. For all three shape factors, the moment of inertia at the apex and bases is I_c=I_b=3671 cm^4, while this value at the eaves ($I_{c\text{-}b}$=$I_{b\text{-}c}$) has values of 3671 cm^4, 4×3671=14684 cm^4 and 8×3671=29368 cm^4, for the shape factors of 0, 2 and 3, respectively. The required parameters for stability matrix with various shape factors, which are presented in Appendix A, have the following values:

$$\bar{l} = \frac{l_b}{l_c} = \frac{1154.70}{1000} = 1.1547 \quad \text{(for } n\text{=0)},$$

$$\bar{a}=\frac{a}{h}=\frac{1000}{2000}=0.5,\ \bar{b}=\frac{b}{h}=\frac{1154.70}{2000}=0.5774,\ \bar{g}=\frac{g}{h}=\frac{2\times1154.70}{2000}=1.1547 \quad \text{(for } n\text{=2 and 3)},$$

$$\alpha=30^{\circ},\ \bar{\mu}=\frac{3671}{3671}=1,\ \bar{K}_{fL}=\bar{K}_{fR}=\bar{K}_f=0.0-1.0,\ \bar{K}_{cL}=\bar{K}_{cR}=\bar{K}_c=1.0,\ \bar{K}_b=0.0-1.0 \quad \text{(for } n\text{=0, 2 and 3)}.$$

Comparisons of the results with those obtained by other available approaches are summarized in Table 6. According to the findings, the proposed method gives a high-accuracy prediction.

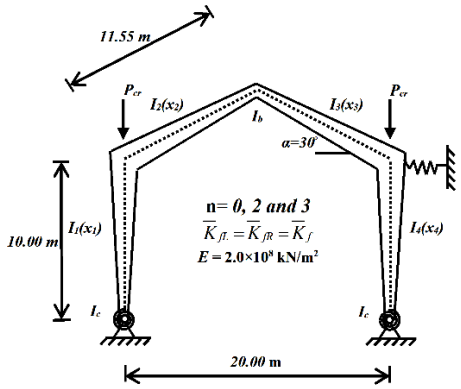

Fig. 6 Geometry and material constants of steel gabled frame with various tapered I-section members and supports (example 4)

Table 6 Comparison of the critical loads, P_{cr} (kN), of the gabled frame in example 4

Type of bases	Bracing system	*n*=0		*n*=2			*n*=3	
		Proposed method	F.E.M (100elements)	Proposed method	Tajmir Riahi *et al*. (2012)	F.E.M. (100elements)	Proposed method	F.E.M. (100elements)
Fixed	Braced	1930.21	1930.24	4024.57	4022.57	4023.73	5634.10	5634.25
Fixed	Unbraced	421.68	421.98	858.68	858.74	858.28	1228.56	1228.63
Hinged	Braced	992.47	992.49	2083.81	2083.94	2083.49	2910.53	2910.66
Hinged	Unbraced	97.62	97.55	280.70	280.73	280.18	461.74	461.77

4. Parametric studies

In this section, the effects of taper ratio, span ratio, flexibility of supports and connections on the equivalent dimensionless critical load factor, $\bar{\rho}_{cr}$, and the corresponding effective length factor, *K*, for three general cases of the steel frames shown in Fig. 7, are studied. It should be noted that the beam-to-column connections in the unbraced frames *A* and *C* are rigid, while frame *B* has semi-rigid connections with 50% rigidity (i.e., $\bar{K}_{cL}=\bar{K}_{cR}=\bar{K}_c=0.5$). For the latter frame, both dimensionless rotational and translational stiffness factors of the foundation and bracing system, are assumed to be 0.5 (i.e., $\bar{K}_{fL}=\bar{K}_{fR}=\bar{K}_f=\bar{K}_b=0.5$). Frame *A* has two hinged supports, while frame *C* is based on fixed foundations. As it will be demonstrated later, parametric studies reveal the pronounced influence of the foregoing parameters.

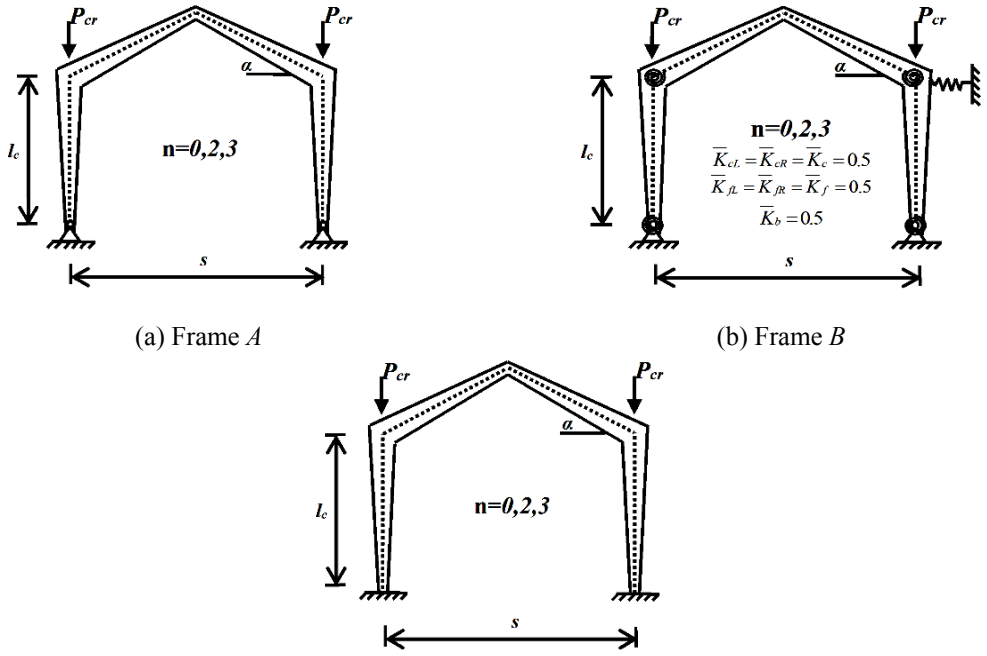

(a) Frame *A*

(b) Frame *B*

(c) Frame *C*

Fig. 7 General forms of frames in the parametric studies

4.1 Effect of taper ratio

According to Eq. (1), the variations of moment inertia, along the length of tapered I-section member have the following form:

$$\left.\begin{aligned} I_i(x_i) &= I_c\left(\frac{x_i}{a}\right)^n = I_c\left(\frac{l_c}{a}\times\frac{x_i}{l_c}\right)^n = I_c\left(c_c\times\frac{x_i}{l_c}\right)^n \qquad (i=1,4)\\ I_j(x_j) &= I_b\left(\frac{x_j}{b}\right)^n = I_b\left(\frac{l_b}{b}\times\frac{x_j}{l_b}\right)^n = I_b\left(c_b\times\frac{x_j}{l_b}\right)^n \qquad (j=2,3)\end{aligned}\right\} \tag{16}$$

Where c_c and c_b are the taper ratios of column and beam, respectively. The taper ratios vary within the range of $0\le c_c$ or $c_b<\infty$, where c_c or $c_b=0$ denote a uniform member. If c_c or $c_b=\infty$, the member would taper to a point at the eave, which is only a theoretical limit and not practical.

Tables 7-9, show the influence of the taper ratio, $c_c=c_b$, on the equivalent effective length factor, K, of frames A, B and C, respectively, for various values of stiffness ratio $\overline{\mu}$ and shape factor n. It is reminded that the stiffness ratio is the ratio of the column moment of inertia at the base, I_c, to the beam moment of inertia at the apex, I_b. Obviously, whenever the taper ratio or the shape factor increases, the equivalent effective length factor of column in frames B and C increases, while it decreases for frame A. Nevertheless, the variation of the taper ratio is more significant for frame B. According to Table 8, as the taper ratio increases from 0.1 to 1.0, the equivalent effective length factor increases by 65%, 63% and 35%, for n=3 and stiffness ratio 0.1, 1.0 and 10, respectively.

Furthermore, it is noticed that irrespective of the taper ratio and shape factor, the equivalent effective length factor reduces as the values of the stiffness ratio increase. This effect is significant for the frame *A*.

Table 7 Influences of the taper ratio c_c=c_b on the equivalent effective length factor *K* with various values of stiffness ratio $\bar{\mu}$ for *n*=2 and *n*=3 in frame *A*

	n=2			*n*=3		
	$\bar{\mu}$=0.1	$\bar{\mu}$=1	$\bar{\mu}$=10	$\bar{\mu}$=0.1	$\bar{\mu}$=1	$\bar{\mu}$=10
0.1	7.420	2.865	2.055	6.778	2.772	2.035
0.2	6.767	2.756	2.021	6.629	2.703	1.988
0.3	6.653	2.712	1.994	6.470	2.641	1.951
0.4	6.556	2.674	1.971	6.337	2.590	1.921
0.5	6.473	2.642	1.952	6.225	2.548	1.896
0.6	6.400	2.614	1.935	6.130	2.512	1.877
0.7	6.337	2.590	1.921	6.049	2.482	1.861
0.8	6.281	2.569	1.909	5.979	2.457	1.848
0.9	6.231	2.551	1.899	5.919	2.435	1.838
1.0	6.187	2.534	1.890	5.867	2.416	1.830

Table 8 Influences of the taper ratio c_c=c_b on the equivalent effective length factor *K* with various values of stiffness ratio $\bar{\mu}$ for *n*=2 and *n*=3 in frame *B*

	n=2			*n*=3		
	$\bar{\mu}$=0.1	$\bar{\mu}$=1	$\bar{\mu}$=10	$\bar{\mu}$=0.1	$\bar{\mu}$=1	$\bar{\mu}$=10
0.1	2.877	2.427	1.692	2.945	2.480	1.708
0.2	3.005	2.528	1.725	3.140	2.635	1.761
0.3	3.130	2.628	1.760	3.340	2.796	1.816
0.4	3.256	2.729	1.795	3.545	2.962	1.876
0.5	3.382	2.831	1.832	3.754	3.132	1.938
0.6	3.507	2.933	1.870	3.968	3.308	2.005
0.7	3.633	3.035	1.908	4.187	3.487	2.074
0.8	3.759	3.138	1.947	4.409	3.671	2.147
0.9	3.885	3.242	1.987	4.636	3.858	2.223
1.0	4.012	3.345	2.027	4.867	4.049	2.303

4.2 Effect of span ratio

The equivalent effective length factor, *K,* of the frames *A*, *B* and *C*, for different values of shape factor, frame slope and span ratio are tabulated in Tables 10-12, respectively. It should be noted that the span ratio, $\bar{s}$, is the ratio of the column height, l_c, to the frame span, *s*. Moreover, it is assumed for all frames that the stiffness ratio is $\bar{\mu}$=1 and the taper ratios are c_c=c_b=1.

According to Tables 10-12, it is observed that the equivalent effective length factor, for all three frames, increases when the span ratio increases. This effect is more pronounced for frame *A*, such that when the span ratio increases from 1.0 to 4.0, the equivalent effective length factor

Table 9 Influences of the taper ratio c_c=c_b on the equivalent effective length factor K with various values of stiffness ratio $\overline{\mu}$ for n=2 and n=3 in frame C

	n=2			n=3		
	$\overline{\mu}$=0.1	$\overline{\mu}$=1	$\overline{\mu}$=10	$\overline{\mu}$=0.1	$\overline{\mu}$=1	$\overline{\mu}$=10
0.1	1.866	1.360	1.048	1.902	1.361	1.048
0.2	1.914	1.372	1.049	1.945	1.378	1.051
0.3	1.943	1.379	1.052	1.992	1.389	1.055
0.4	1.973	1.387	1.055	2.040	1.401	1.060
0.5	2.002	1.395	1.059	2.089	1.413	1.065
0.6	2.032	1.403	1.063	2.137	1.425	1.071
0.7	2.061	1.411	1.067	2.185	1.438	1.078
0.8	2.089	1.419	1.072	2.233	1.450	1.085
0.9	2.117	1.428	1.076	2.281	1.462	1.092
1.0	2.145	1.436	1.081	2.328	1.474	1.100

Table 10 Influences of the span ratio $\overline{s}$ on the equivalent effective length factor K with various values of shape factor and frame slope for $\overline{\mu}$=1 and c_c=c_b=1 in frame A

	n=0			n=2			n=3		
	α=15°	α=30°	α=45°	α=15°	α=30°	α=45°	α=15°	α=30°	α=45°
1.0	2.339	2.377	2.458	2.088	2.119	2.186	2.007	2.035	2.096
1.5	2.500	2.555	2.670	2.222	2.267	2.364	2.128	2.170	2.259
2.0	2.655	2.724	2.870	2.351	2.410	2.534	2.247	2.301	2.416
2.5	2.804	2.886	3.060	2.477	2.548	2.696	2.364	2.429	2.568
3.0	2.946	3.041	3.240	2.599	2.680	2.851	2.477	2.553	2.712
3.5	3.083	3.189	3.411	2.716	2.808	2.999	2.586	2.672	2.851
4.0	3.214	3.332	3.575	2.829	2.931	3.141	2.692	2.787	2.985

Table 11 Influences of the span ratio $\overline{s}$ on the equivalent effective length factor K with various values of shape factor and frame slope for $\overline{\mu}$=1 and c_c=c_b=1 in frame B

	n=0			n=2			n=3		
	α=15°	α=30°	α=45°	α=15°	α=30°	α=45°	α=15°	α=30°	α=45°
1.0	1.989	2.026	2.095	2.738	2.807	2.936	3.273	3.363	3.530
1.5	2.128	2.166	2.235	2.995	3.062	3.184	3.605	3.692	3.846
2.0	2.227	2.264	2.331	3.170	3.233	3.345	3.828	3.908	4.049
2.5	2.302	2.337	2.399	3.297	3.356	3.459	3.989	4.063	4.191
3.0	2.360	2.393	2.451	3.394	3.449	3.543	4.110	4.178	4.295
3.5	2.407	2.438	2.492	3.471	3.522	3.609	4.205	4.268	4.376
4.0	2.445	2.474	2.525	3.533	3.580	3.660	4.282	4.340	4.439

increases by about 37%, 40% and 45%, in the uniform gabled frame, for α=15°, 30° and 45°, respectively. In addition, as the frame slope increases, regardless of the span ratio and shape factor, the equivalent effective length factor of the frame increases. Furthermore, irrespective of the value of $\overline{s}$, when the shape factor increases, the equivalent effective length factor decreases, in frame A, while increases in frames B and C.

Table 12 Influences of the span ratio $\bar{s}$ on the equivalent effective length factor K with various values of shape factor and frame slope for $\bar{\mu}$=1 and c_c=c_b=1 in frame C

	n=0			n=2			n=3		
	α=15°	α=30°	α=45°	α=15°	α=30°	α=45°	α=15°	α=30°	α=45°
1.0	1.161	1.178	1.212	1.204	1.223	1.261	1.226	1.245	1.285
1.5	1.229	1.250	1.292	1.281	1.305	1.355	1.306	1.332	1.386
2.0	1.287	1.311	1.358	1.349	1.378	1.436	1.379	1.411	1.474
2.5	1.337	1.363	1.413	1.410	1.442	1.505	1.446	1.481	1.552
3.0	1.381	1.408	1.460	1.464	1.499	1.565	1.506	1.544	1.619
3.5	1.420	1.447	1.499	1.513	1.549	1.618	1.561	1.601	1.679
4.0	1.454	1.482	1.534	1.557	1.594	1.664	1.610	1.652	1.733

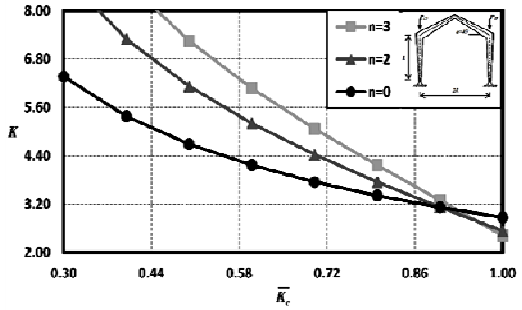

(a) Frame A

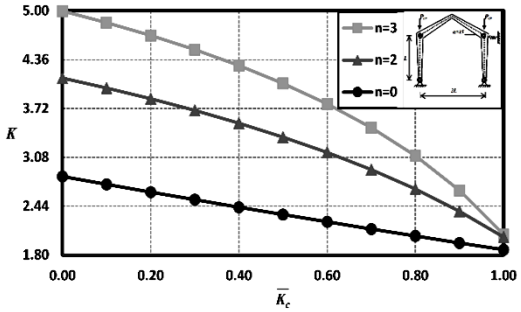

(b) Frame B

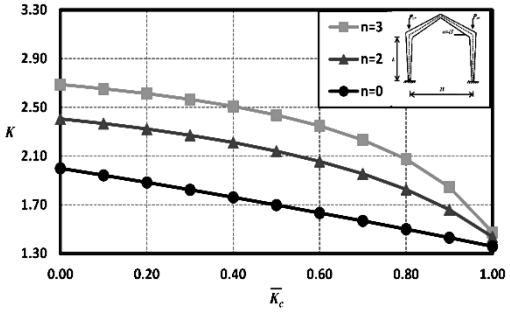

(c) Frame C

Fig. 8 Influence of the non-dimensional rotational stiffness factor of the semi-rigid connection $\overline{K}_c$ on the equivalent effective length factor K ($\overline{K}_{cL} = \overline{K}_{cR} = \overline{K}_c$ and $\bar{\mu} = 1$)

4.3 Effect of semi-rigid beam-to-column connections

The influences of the non-dimensional rotational stiffness factor of the semi-rigid connection, $\overline{K}_c$, on the equivalent effective length factor of column, K, and corresponding dimensionless equivalent critical load factor, $\overline{\rho}_{cr}$, for frames A, B and C, are depicted in Figs. 8 and 9, respectively. It is assumed for each frame that; the column height l_c=L, span of the frame s=2L and the frame slope α=45°. In addition, the non-dimensional rotational stiffness factor of the semi-rigid

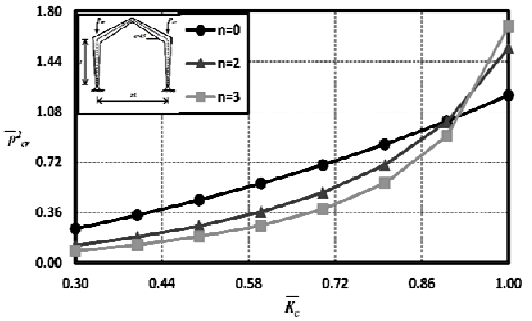

(a) Frame *A*

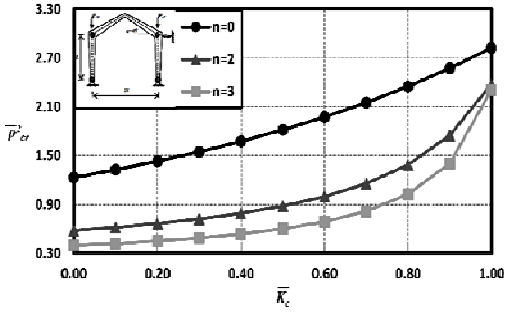

(b) Frame *B*

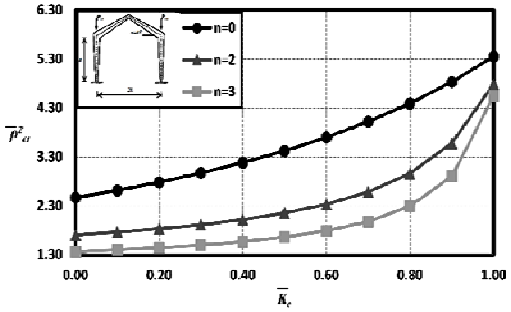

(c) Frame *C*

Fig. 9 Effect of the non-dimensional rotational stiffness of the semi-rigid connection factor $\overline{K}_c$ on the dimensionless equivalent critical load factor $\overline{\rho}_{cr}^2$ ($\overline{K}_{cL} = \overline{K}_{cR} = \overline{K}_c$ and $\overline{\mu} = 1$)

connection varies within the range of 0 to 1. A value of $\overline{K}_c = 0.0$ represents a pinned connection, whereas $\overline{K}_c = 1.0$ indicates that the connection of beam-to-column is rigid.

Based on the Figs. 8 and 9, it is evident that as $\overline{K}_c$ increases, the value of K decreases, while the corresponding dimensionless equivalent critical load factor, $\overline{\rho}_{cr}$, increases. Fig. 8(a) indicates that when $\overline{K}_c$ increases from 0.0 to 1.0, the equivalent effective length factor of column reduces by about 96%, 94% and 92%, for n=3, 2 and 0, respectively. Furthermore, as the shape factor, n, increases, the equivalent effective length factor increases in frames *B* and *C*, while this effect reverses when the values of $\overline{K}_c$ exceed 0.90 in the frame *A*. Similarly, according to Fig. 9, the value of $\overline{\rho}_{cr}$ for the corresponding gabled frame with uniform members (i.e., I_c=I_m), is always greater than that of the gabled frame with tapered members, except for the values of $\overline{K}_c$ exceeding 0.90 in the frame *A*. In other words, the load-carrying capacity of the gabled frame with tapered members, is not greater than the corresponding gabled frame with uniform members. It should be mentioned that for all connection flexibilities, the load-carrying capacity of the gabled frame *C* is more than those of other frames.

4.4 Effect of elastic translational restraint

In Figs. 10 and 11, the effects of the non-dimensional translational stiffness factor of the brace, $\overline{K}_b$, on the equivalent effective length factor of column, K, and the corresponding equivalent

dimensionless buckling load factor, $\overline{\rho}_{cr}$, for frames *A*, *B* and *C*, are investigated, respectively. It should be noted that $\overline{K}_b$ varies within the range of $\overline{K}_b$ = 0.0 (i.e., unbraced frame) to $\overline{K}_b$ = 1.0 (i.e., braced frame). Moreover, it is assumed for both frames that the column height, span and slope of the frame are l_c=L, s=2L and α=45°, respectively.

According to the Figs. 10 and 11, it is obvious that the equivalent effective length factor of column in gabled frames, *K*, decreases and the corresponding equivalent dimensionless buckling load factor, $\overline{\rho}_{cr}$, increases, when $\overline{K}_b$ increases. This influence is more pronounced for frame *B*, as shown in Fig. 10(b). As $\overline{K}_b$ increases from 0.0 to 1.0, the equivalent effective length factor of column decreases by about 78%, 75% and 68%, for n=3, 2 and 0, respectively. In addition, when the shape factor, n, increases, the equivalent effective length factor increases in frames *B* and *C*, while this effect reverses when the values of $\overline{K}_b$ are smaller than 0.55 in the frame *A*. Similarly, Fig. 11 indicates that the value of the dimensionless equivalent critical load factor, $\overline{\rho}_{cr}$, for the corresponding gabled frame with uniform members (i.e., I_c=I_m), is always greater than that of the gabled frame with tapered members, except for values of $\overline{K}_b$ below 0.55 in the frame *A*. In fact; the load-carrying capacity of the gabled frame with tapered members, is smaller than the corresponding gabled frame with uniform members having the same values of $\overline{K}_b$. Nevertheless, the non-dimensional equivalent critical load factor increases only slightly when $\overline{K}_b$ is smaller than 0.50. Moreover, the load-carrying capacity of gabled frame *C* is more than other frames, for all values of $\overline{K}_b$.

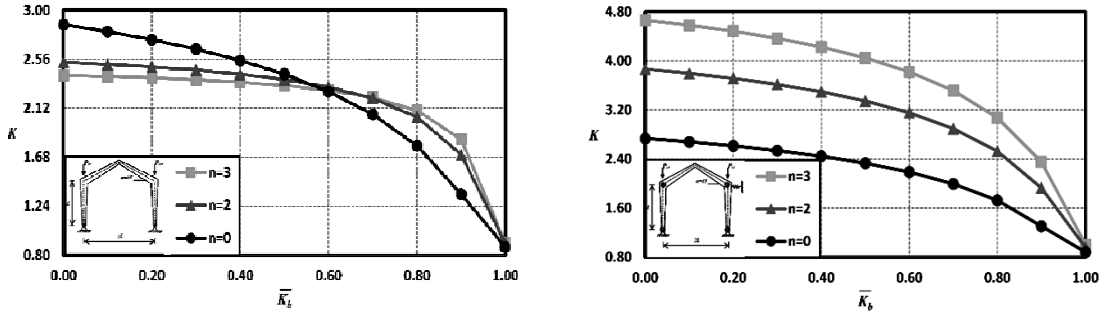

(a) Frame *A*

(b) Frame *B*

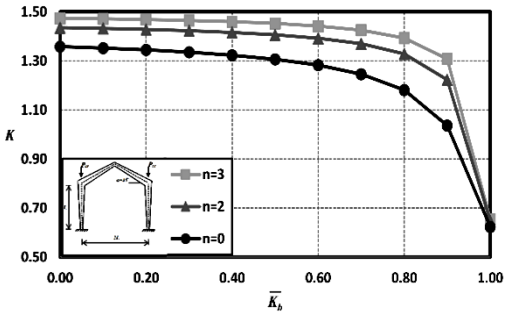

(c) Frame *C*

Fig. 10 Influence of the non-dimensional translational stiffness factor of the brace $\overline{K}_b$ on the equivalent effective length factor *K* ($\overline{\mu}$ = 1)

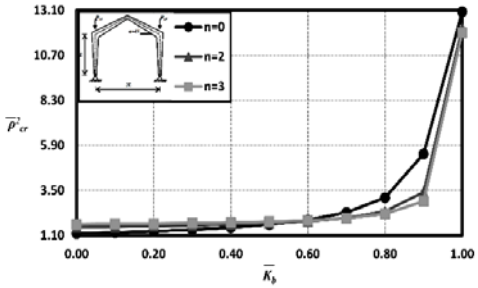

(a) Frame *A*

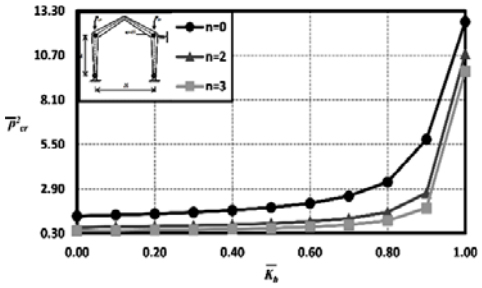

(b) Frame *B*

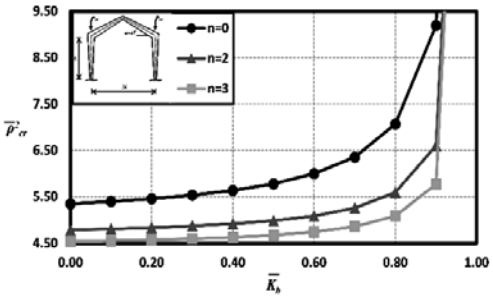

(c) Frame *C*

Fig. 11 Effect of the non-dimensional translational stiffness factor of the brace $\overline{K}_b$ on the dimensionless equivalent critical load factor $\overline{\rho}_{cr}^2$ ($\overline{\mu} = 1$)

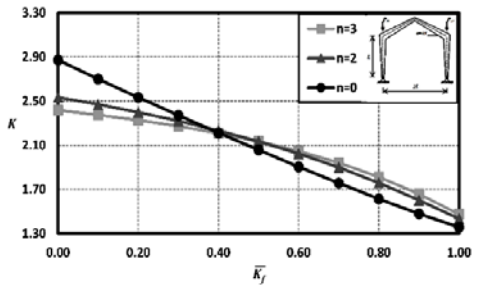

(a) Frame *A*

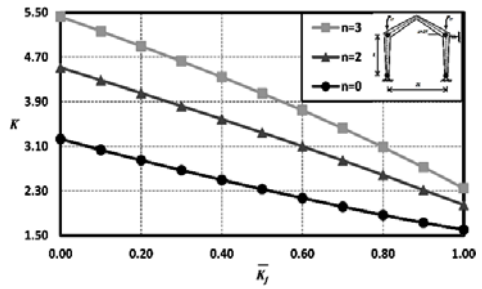

(b) Frame *B*

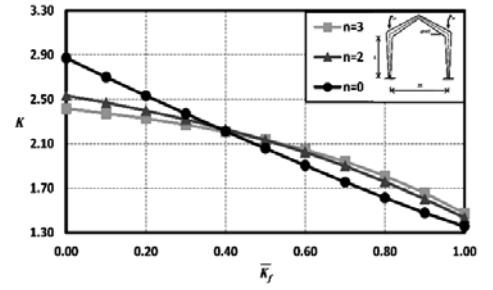

(c) Frame *C*

Fig. 12 Influence of the non-dimensional rotational stiffness factor of the foundation $\overline{K}_f$ on the equivalent effective length factor K ($\overline{K}_{fL} = \overline{K}_{fR} = \overline{K}_f$ and $\overline{\mu} = 1$)

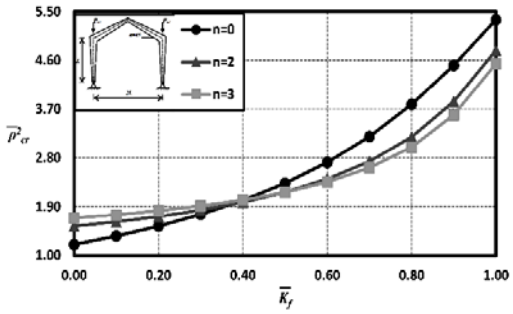

(a) Frame *A*

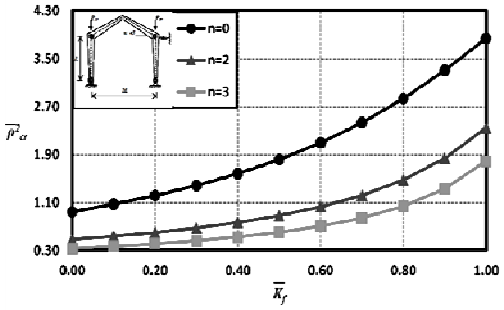

(b) Frame *B*

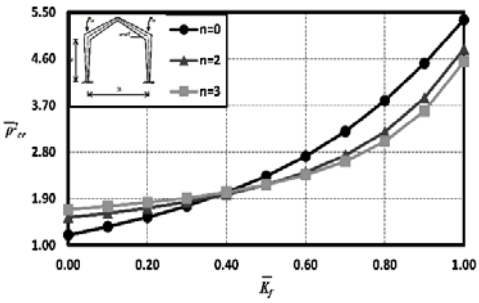

(c) Frame *C*

Fig. 13 Effect of the non-dimensional rotational stiffness factor of the foundation $\overline{K}_f$ on the dimensionless equivalent critical load factor $\overline{\rho}_{cr}^2$ ($\overline{K}_{fL} = \overline{K}_{fR} = \overline{K}_f$ and $\overline{\mu} = 1$)

4.5 Effect of elastic rotational restraints

The influences of the non-dimensional rotational stiffness factor of the foundation, $\overline{K}_f$, on the equivalent effective length factor of column, *K*, and the corresponding equivalent dimensionless critical load factor, $\overline{\rho}_{cr}$, for the frames *A*, *B* and *C*, are shown in Figs. 12 and 13, respectively. It is reminded that $\overline{K}_f$ varies within the range of 0 to 1. The value of $\overline{K}_f$=0.0 represents hinged supports and $\overline{K}_f$=1.0, represents fixed bases. Furthermore, it is assumed that the column height l_c=L, span of the frame s=2L and the frame slope α=45°, for each frame.

From Figs. 12 and 13, it is observed that as $\overline{K}_f$ increases, the equivalent effective length factor, *K*, decreases linearly, while the corresponding dimensionless equivalent critical load factor, $\overline{\rho}_{cr}$, increases. The flexibility of foundations is more considerable for frame *B*. Fig. 12(b) shows that when $\overline{K}_f$ increases from 0.0 to 1.0, the equivalent effective length factor of column decreases by about 57%, 55% and 50%, for n=3, 2 and 0, respectively. In addition, as the shape factor, *n*, increases, the equivalent effective length factor increases in frame *B*, while this effect reverses for the values of $\overline{K}_f$ less than 0.40, for both frames *A* and *C*. Similarly, according to Fig. 13, the dimensionless equivalent critical load factor, $\overline{\rho}_{cr}$, for the corresponding gabled frame with uniform members (i.e., I_c=I_m), is always greater than that of the gabled frame with tapered members, except for the values of $\overline{K}_f$ less than 0.40 in frame *A*. In other words, the load-arrying capacity of the gabled frame with uniform members, is greater than the corresponding gabled frame with tapered members.

5. Conclusions

This paper tackles buckling analysis of a general gabled frame with different I-section members. Based on the Euler-Bernoulli beam-column theory, the governing fourth-order differential equation was accurately solved and the stability matrix for a semi-rigid frame, with prismatic and/or non-prismatic members and elastic supports, was obtained. It was assumed that the semi-rigid connections and elastic supports have a linear behavior, and both were modeled by linear springs. The moment of inertia variations over the length of non-uniform members was assumed to be cubic for I-section element with linearly varying amplitudes of web and flanges. On the other hand, it was modeled as parabolic functions for web-tapered. The presented formulation can exactly determine the critical load, and corresponding equivalent effective length factor of uniform and/or non-uniform gabled frames with semi-rigid connections and elastic supports. Comparing the available literature results with the current approach demonstrates the accuracy, efficiency and capabilities of the proposed method. Parametric studies for gabled frames disclose the effects of the taper ratio, shape factor, stiffness ratio, frame slope, span ratio, flexibility of connections and elastic supports on the dimensionless equivalent buckling load factor of structures, and corresponding equivalent effective length factor of the gabled frames. With regard to the findings of this study, the following points are concluded:

• The influences of the flexibility of connections, lateral stiffness of bracing system, taper ratio, rigidity of foundations, and the span ratio on the critical load and corresponding equivalent effective length factor of frames are very significant. In some cases, they can decrease the columns' effective length factor by about 96%, 78%, 65%, 57% and 45%, respectively. Accordingly, these effects should be considered in stability design of gabled frames.

• As the non-dimensional factors of rotational stiffness of the semi-rigid connection; translational stiffness of the brace; and rotational stiffness of the foundation increase, the equivalent effective length factor, K, decreases, while the corresponding dimensionless equivalent critical load factor, $\overline{\rho}_{cr}$, increases.

• The load-carrying capacity of the gabled frame with tapered members, for most cases, is less than the corresponding gabled frame with uniform members.

• The effect of variation of the taper ratio is more pronounced for gabled frame with flexible connections and supports. Irrespective of the taper ratio and shape factor, the equivalent effective length factor decreases, when the stiffness ratio increases.

• As the span ratio increases, the equivalent effective length factor of the gabled frame increases. When the frame slope increases, regardless of the span ratio and shape factor, the equivalent effective length factor of the frame increases.

• The flexibility of connections has a very significant effect on unbraced frame with hinged bases. In fact, for this structure, as the shape factor, n, increases, the equivalent effective length factor increases, while this effect reverses for the values of $\overline{K}_c$ greater than 0.9, and for the values of $\overline{K}_b$ and $\overline{K}_f$ smaller than 0.55 and 0.4, respectively.

• Increasing of the non-dimensional equivalent critical load factors is negligible when the non-dimensional translational stiffness factor of the bracing system is less than 0.5.

References

AISC (1999), Load and Resistance Factor Design Specification, for Structural Steel Building, American Institute of Steel Construction, December, USA.

Al-Sadder, S.Z. (2004), "Exact expressions for stability functions of a general non-prismatic beam-column member", *J. Constr. Steel Res*., **60**(11), 1561-1584.

Bazant, Z.P. (2000), "Structural stability", *Int. J. Solid. Struct*., **37**(1-2), 55-67.

Chan, S., Huang, H. and Fang, L. (2005), "Advanced analysis of imperfect portal frames with semirigid base connections", *J. Eng. Mech*., **131**(6), 633-640.

Cristutiu, I. and Nunes, D. (2013a), "Behaviour of pitched-roof portal frames with tapered web and flange members considering lateral restraints", *Proceedings of the Fifth International Conference on Structural Engineering, Mechanics and Computation SEMC2013*, Cape Town, South Africa, September.

Cristutiu, I.M. and Nunes, D.L. (2013b), "Advanced FEM analysis of steel pitched-roof portal frames with tapered members", *Adv. Mater. Res*., **710**(June), 358-361.

Essa, H.S. (1998), "New stability equation for columns in unbraced frames", *Struct. Eng. Mech*., **6**(4), 411-425.

Fraser, D.J. (1980), "Effective lengths in gable frames, sways not prevented", *Civil Eng. Tran*., **19**(2), 176-183.

Fraser, D.J. (1983), "Design of tapered member portal frames", *J. Constr. Steel Res*., **3**(3), 20-26.

Hayalioglu, M.S. and Saka, M.P. (1992), "Optimum design of geometrically nonlinear elastic-plastic steel frames with tapered members", *Comput. Struct*., **44**(4), 915-924.

Hwang, J., Chang, K., Lee, G. and Ketter, R. (1989), "Shaking table tests of pinned-base steel gable frame", *J. Struct. Eng*., **115**(12), 3031-3043.

Hwang, J.S., Chang, K.C. and Lee, G.C. (1991), "Seismic behavior of gable frame consisting of tapered members", *J. Struct. Eng*., **117**(3), 808-821.

Irani, F. (1988), "Stability of one bay symmetrical frames with nonuniform members", *Int. J. Eng*., **1**(4), 193-200.

Issa, H.K. and Mohammad, F.A. (2009), "Practical non-prismatic stiffness matrix for haunched-rafter of pitched-roof steel portal frames", *Challenges, opportunities, and solutions in structural engineering and construction*, ISEC-5.

Karabalis, D.L. and Beskos, D.E. (1983), "Static, dynamic and stability analysis of structures composed of tapered beams", *Comput. Struct*., **16**(6), 731-748.

Lee, G.C. and Morrell, M.L. (1975), "Application of AISC design provisions for tapered members", *Eng. J*., 12, 1-13.

Lee, G.C., Morrell, M.L. and Ketter, R.L. (1971), "Design of tapered members", No. 173, Welding Research Council Bulletin.

Li, G.Q. and Li, J.J. (2000), "Effects of shear deformation on the effective length of tapered columns with I-section for steel portal frames", *Struct. Eng. Mech*., **10**(5), 479-489.

Li, G.Q. and Li, J.J. (2002), "A tapered Timoshenko-Euler beam element for analysis of steel portal frames", *J. Constr. Steel Res*., **58**(12), 1531-1544.

Li, J.J. and Li, G.Q. (2004), "Reliability-based integrated design of steel portal frames with tapered members", *Struct. Saf*., **26**(2), 221-239.

Li, J.J., Li, G.Q. and Chan, S.L. (2003), "A second-order inelastic model for steel frames of tapered members with slender web", *Eng. Struct*., **25**(8), 1033-1043.

Li, J., Wang, Y.Q., Chang, T. and Shi, F. (2011), "In-Plane buckling analysis of gabled arch frame steel building", *Appl. Mech. Mater*., **71-78**, 3680-3686.

Liao, X.J., Shi, Y.J. and Wang, Y.Q. (2005), "The analysis of steel gabled frames with flexible connections", *Proceeding of the Fourth International Conference on Advances in Steel Structures*, Shanghai, China, June.

Lu, L. (1964), "Effective length of columns in gable frames", *Eng. J*., AISC, **2**(1), 1-6.

Manolis, G.D., Beskos, D.E. and Brand, B.J. (1986), "Elastoplastic analysis and design of gabled frames", *Comput. Struct*., **22**(4), 693-697.
Marques, L., da Silva, L.S. and Rebelo, C. (2014), "Rayleigh-Ritz procedure for determination of the critical load of tapered columns", *Steel Compos. Struct*., **16**(1), 47-60.
Miller, C.J. and Moll Jr., T.G. (1979), "Automatic design of tapered member gabled frames", *Comput. Struct*., **10**(6), 847-854.
Mohamed, S.E. and Simitses, G.J. (1989), "Buckling of flexibly-connected gabled frames", *Int. J. Nonlin. Mech*., **24**(5), 353-364.
Mohamed, S.E., Kounadis, A.N. and Simitses, G.J. (1991), "Elastic-plastic instability of flexibly connected non-orthogonal frames", *Comput. Struct*., **39**(6), 663-669.
Mohamed, S.E., Kounadis, A.N. and Simitses, G.J. (1992), "Elasto-plastic analysis of gabled frames with nonprismatic geometries", *Comput. Struct*., **44**(3), 693-697.
Papadopoulos, P.G., Papadopoulou, A.K. and Papaioannou, K.K. (2008), "Simple nonlinear static analysis of steel portal frame with pitched roof exposed to fire", *Struct. Eng. Mech*., **29**(1), 37-53.
Rezaiee-Pajand, M. (1990), "Gable frame analysis using iteration procedure", *Amirkabir*, **4**, 41-61.
Ronagh, H.R. and Bradford, M.A. (1996), "A rational model for the distortional buckling of tapered members", *Comput. Meth. Appl. Mech. Eng*., **130**(3-4), 263-277.
Safavi, A.A. and Moharami, H. (2009), "Coefficient of effective length of tapered columns in one-bay gabled frames for state of free to sway with hinged bases", *Sharif Civ. Eng*., **25**(48), 22-30. (in Persian)
Saffari, H., Rahgozar, R. and Jahanshahi, R. (2008), "An efficient method for computation of effective length factor of columns in a steel gabled frame with tapered members", *J. Constr. Steel Res*., **64**(4), 400-406.
Saka, M.P. (1997), "Optimum design of steel frames with tapered members", *Comput. Struct*., **63**(4), 797-811.
Shooshtari, A. and Khajavi, R. (2010), "An efficient procedure to find shape functions and stiffness matrices of nonprismatic Euler-Bernoulli and Timoshenko beam elements", *Eur. J. Mech. Solid.*, **29**(5), 826-836.
Silvestre, N. and Camotim, D. (2005), "Second-order analysis and design of pitched-roof steel frames", *Proceeding of the Fourth International Conference on Advances in Steel Structures*, Shanghai, China, June.
Silvestre, N. and Camotim, D. (2007), "Elastic buckling and second-order behaviour of pitched-roof steel frames", *J. Constr. Steel Res*., **63**(6), 804-818.
Silvestre, N., Camotim, D. and Corrêa, M. (1998), "On the design and safety checking of unbraced pitched-roof steel frames", *J. Constr. Steel Res*., **46**(1-3), 328-330.
Silvestre, N., Mesquita, A., Camotim, D. and Silva, L. (2000), "In-plane buckling behavior of pitched-roof steel frames with semi-rigid connections", *In Frames with Partially Restrained Connections*, SSRC 1998 Theme Conference Workshop Volume, 21-34.
Simitses, G.J. and Mohamed, S.E. (1989), "Nonlinear analysis of gabled frames under static loads", *J. Constr. Steel Res*., **12**(1), 1-17.
Simitses, G.J. and Mohamed, S.E. (1990), "Instability and collapse of flexibly-connected gabled frames", *Int. J. Solid. Struct*., **26**(9-10), 1159-1171.
Tajmir Riahi, H., Shojaei Barjoui, A., Bazazzadeh, S. and Etezady, S.M.A. (2012), "Buckling analysis of non-prismatic columns using slope-deflection method", *Proceedings of the 15th World Conference on Earthquake Engineering 15WCEE*, Lisbon, Portugal, September.
Vlahinos, A.S. and Cervantes, A. (1990), "Buckling and postbuckling behaviour of gabled frames", *Math. Comput. Model*., **14**, 873-876.
Wang, J.F. and Li, G.Q. (2007), "Stability analysis of semi-rigid composite frames", *Steel Compos. Struct*., **7**(2), 119-133.
Wang, Y., Liu, Y.J. and Xu, Y.F. (2011), "Stiffness analysis on semi-rigid joints in gabled frames", *Adv. Mater. Res*., **243-249**(1), 120-123.
Wilson, J.F. and Strong, D.J. (1997), "Elastic buckling of end-loaded, tapered, cantilevered beams with initial curvature", *Struct. Eng. Mech*., **5**(3), 257-268.

Xu, D., Zhang, Q. and Liu, S. (2010), "Research on the effective length factor of tapered gable portal frames with leaning columns", *Struct. Eng*., **3**, 66-71. (in Chinese)
Yuan, Z. (2004), "Advanced analysis of steel frame structures subjected to lateral torsional buckling effects", Ph.D. Dissertation, Queensland University of Technology, Australia.

CC

Appendix A

The unknown constants' matrix, **K** for the frame has the below form:

$$\mathbf{K}=\begin{bmatrix}
K_{1,1} & K_{1,2} & K_{1,3} & K_{1,4} & 0 & 0 & 0 & 0 & 0 & 0 & 0 & 0 & 0 & 0 & 0 & 0\\
K_{2,1} & K_{2,2} & K_{2,3} & 0 & 0 & 0 & 0 & 0 & 0 & 0 & 0 & 0 & 0 & 0 & 0 & 0\\
0 & 0 & 0 & 0 & 0 & 0 & 0 & 0 & 0 & 0 & 0 & 0 & K_{3,13} & K_{3,14} & K_{3,15} & K_{3,16}\\
0 & 0 & 0 & 0 & 0 & 0 & 0 & 0 & 0 & 0 & 0 & 0 & K_{4,13} & K_{4,14} & K_{4,15} & 0\\
K_{5,1} & K_{5,2} & K_{5,3} & K_{5,4} & K_{5,5} & K_{5,6} & K_{5,7} & K_{5,8} & 0 & 0 & 0 & 0 & 0 & 0 & 0 & 0\\
K_{6,1} & K_{6,2} & K_{6,3} & K_{6,4} & K_{6,5} & K_{6,6} & K_{6,7} & K_{6,8} & 0 & 0 & 0 & 0 & 0 & 0 & 0 & 0\\
0 & 0 & 0 & 0 & 0 & 0 & 0 & 0 & K_{7,9} & K_{7,10} & K_{7,11} & K_{7,12} & K_{7,13} & K_{7,14} & K_{7,15} & K_{7,16}\\
0 & 0 & 0 & 0 & 0 & 0 & 0 & 0 & K_{8,9} & K_{8,10} & K_{8,11} & K_{8,12} & K_{8,13} & K_{8,14} & K_{8,15} & K_{8,16}\\
K_{9,1} & K_{9,2} & K_{9,3} & K_{9,4} & 0 & 0 & 0 & 0 & 0 & 0 & 0 & 0 & K_{9,13} & K_{9,14} & K_{9,15} & K_{9,16}\\
0 & 0 & K_{10,3} & 0 & 0 & 0 & 0 & 0 & 0 & 0 & 0 & 0 & K_{10,13} & K_{10,14} & K_{10,15} & K_{10,16}\\
K_{11,1} & K_{11,2} & 0 & 0 & K_{11,5} & K_{11,6} & 0 & K_{11,8} & 0 & 0 & 0 & 0 & 0 & 0 & 0 & 0\\
K_{12,1} & K_{12,2} & K_{12,3} & 0 & 0 & K_{12,6} & K_{12,7} & K_{12,8} & 0 & 0 & 0 & 0 & 0 & 0 & 0 & 0\\
0 & 0 & 0 & 0 & 0 & 0 & 0 & 0 & K_{13,9} & K_{13,10} & 0 & K_{13,12} & K_{13,13} & K_{13,14} & 0 & 0\\
0 & 0 & 0 & 0 & 0 & 0 & 0 & 0 & K_{14,9} & K_{14,10} & K_{14,11} & K_{14,12} & K_{14,13} & K_{14,14} & K_{14,15} & 0\\
0 & 0 & 0 & 0 & 0 & K_{15,6} & 0 & K_{15,8} & 0 & K_{15,10} & 0 & K_{15,12} & 0 & 0 & 0 & 0\\
0 & 0 & 0 & 0 & K_{16,5} & K_{16,6} & K_{16,7} & K_{16,8} & K_{16,9} & K_{16,10} & K_{16,11} & K_{16,12} & 0 & 0 & 0 & 0
\end{bmatrix} \tag{A-1}$$

For the shape factor n=0, the entries of the unknown constants' matrix are as follows:

$$K_{1,1}=K_{1,3}=K_{3,13}=K_{3,15}=K_{5,5}=K_{5,6}=K_{5,7}=K_{7,9}=K_{7,10}=K_{7,11}=K_{11,8}=K_{13,12}=K_{15,8}=K_{15,12}=$$
$$K_{16,5}=K_{16,6}=K_{16,8}=K_{16,9}=K_{16,10}=K_{16,12}=0 \tag{A-2}$$

$$K_{1,2}=K_{1,4}=K_{3,14}=K_{3,16}=K_{9,3}=K_{9,4}=-K_{9,15}=-K_{9,16}=-K_{15,6}=-K_{15,10}=K_{16,7}=-K_{16,11}=1 \tag{A-3}$$

$$K_{2,1}=\overline{K}_{fL}\rho \tag{A-4}$$

$$K_{2,2}=\rho^2\left(1-\overline{K}_{fL}\right) \tag{A-5}$$

$$K_{2,3}=\overline{K}_{fL} \tag{A-6}$$

$$K_{4,13}=\overline{K}_{fR}\rho \tag{A-7}$$

$$K_{4,14}=\rho^2\left(1-\overline{K}_{fR}\right) \tag{A-8}$$

$$K_{4,15}=\overline{K}_{fR} \tag{A-9}$$

$$K_{5,1}=K_{6,1}=K_{7,13}=K_{8,13}=-\sin\rho\sin\alpha \tag{A-10}$$

$$K_{5,2}=K_{6,2}=K_{7,14}=K_{8,14}=-\cos\rho\sin\alpha \tag{A-11}$$

$$K_{5,3}=K_{5,4}=K_{6,3}=K_{6,4}=K_{7,15}=K_{7,16}=K_{8,15}=K_{8,16}=-\sin\alpha \tag{A-12}$$

$$K_{5,8}=K_{6,7}=K_{6,8}=K_{7,12}=K_{8,11}=K_{8,12}=\bar{l} \tag{A-13}$$

$$K_{6,5}=K_{8,10}=\bar{l}^3 \tag{A-14}$$

$$K_{6,6} = K_{8,11} = \bar{l}^2 \tag{A-15}$$

$$K_{9,1} = -K_{9,13} = \sin\rho \tag{A-16}$$

$$K_{9,2} = -K_{9,14} = \cos\rho \tag{A-17}$$

$$K_{10,3} = -\rho^2\left(1-\overline{K}_b\right) \tag{A-18}$$

$$K_{10,13} = \overline{K}_b \sin\rho \tag{A-19}$$

$$K_{10,14} = \overline{K}_b \cos\rho \tag{A-20}$$

$$K_{10,15} = \overline{K}_b - \rho^2\left(1-\overline{K}_b\right) \tag{A-21}$$

$$K_{10,16} = \overline{K}_b \tag{A-22}$$

$$K_{11,1} = K_{13,13} = \rho^2 \sin\rho \tag{A-23}$$

$$K_{11,2} = K_{13,14} = \rho^2 \cos\rho \tag{A-24}$$

$$K_{11,5} = K_{13,9} = -6\overline{\mu}\bar{l} \tag{A-25}$$

$$K_{11,6} = K_{13,10} = -2\overline{\mu} \tag{A-26}$$

$$K_{12,1} = -\overline{K}_{cL} \cos\rho \tag{A-27}$$

$$K_{12,2} = \overline{K}_{cL} \sin\rho \tag{A-28}$$

$$-K_{12,3} = K_{12,7} = \overline{K}_{cL} \tag{A-29}$$

$$K_{12,5} = 3\bar{l}^2\left(2-\overline{K}_{cL}\right) \tag{A-30}$$

$$K_{12,6} = K_{14,10} = 2\bar{l} \tag{A-31}$$

$$K_{14,9} = 3\bar{l}^2\left(2-\overline{K}_{cR}\right) \tag{A-32}$$

$$K_{14,11} = -K_{14,15} = \overline{K}_{cR} \tag{A-33}$$

$$K_{14,13} = -\overline{K}_{cR} \cos\rho \tag{A-34}$$

$$K_{14,14} = \overline{K}_{cR} \sin\rho \tag{A-35}$$

The entries of the unknown constants' matrix for the shape factor n=2 can be written as follows:

$$K_{1,1} = K_{3,13} = K_{11,5} = K_{13,9} = K_{14,11} = K_{16,7} = K_{16,11} = 0 \tag{A-36}$$

$$K_{5,7}=K_{6,7}=K_{7,11}=K_{8,11}=K_{9,3}=K_{9,4}=-K_{9,15}=-K_{9,16}=-K_{15,6}=-K_{15,10}=K_{16,5}=-K_{16,9}=1 \quad \text{(A-37)}$$

$$K_{1,2}=K_{3,14}=\sqrt{\bar{a}} \quad \text{(A-38)}$$

$$K_{1,3}=K_{3,15}=\bar{a} \quad \text{(A-39)}$$

$$K_{2,1}=\overline{K}_{fL}\rho\left(1-\bar{a}\right)\sqrt{\bar{a}} \quad \text{(A-40)}$$

$$K_{2,2}=\left[\bar{a}\rho^2\left(1-\overline{K}_{fL}\right)+\left(1-\bar{a}\right)\overline{K}_{fL}/2\right]\sqrt{\bar{a}} \quad \text{(A-41)}$$

$$K_{2,3}=\overline{K}_{fL}\bar{a}\left(1-\bar{a}\right) \quad \text{(A-42)}$$

$$K_{4,13}=\overline{K}_{fR}\rho\left(1-\bar{a}\right)\sqrt{\bar{a}} \quad \text{(A-43)}$$

$$K_{4,14}=\left[\bar{a}\rho^2\left(1-\overline{K}_{fR}\right)+\left(1-\bar{a}\right)\overline{K}_{fR}/2\right]\sqrt{\bar{a}} \quad \text{(A-44)}$$

$$K_{4,15}=\overline{K}_{fR}\bar{a}\left(1-\bar{a}\right) \quad \text{(A-45)}$$

$$K_{5,1}=K_{6,1}=K_{7,13}=K_{8,13}=-\sin\beta\sin\alpha \quad \text{(A-46)}$$

$$K_{5,2}=K_{6,2}=K_{7,14}=K_{8,14}=-\cos\beta\sin\alpha \quad \text{(A-47)}$$

$$K_{5,3}=K_{5,4}=K_{6,3}=K_{6,4}=K_{7,15}=K_{7,16}=K_{8,15}=K_{8,16}=-\sin\alpha \quad \text{(A-48)}$$

$$K_{5,5}=K_{7,9}=\bar{b} \quad \text{(A-49)}$$

$$K_{5,6}=K_{7,10}=\bar{b}\ln\bar{b} \quad \text{(A-50)}$$

$$K_{5,8}=K_{7,12}=\ln\bar{b} \quad \text{(A-51)}$$

$$K_{6,5}=K_{8,9}=\bar{g} \quad \text{(A-52)}$$

$$K_{6,6}=K_{8,10}=\bar{g}\ln\bar{g} \quad \text{(A-53)}$$

$$K_{6,8}=K_{8,12}=\ln\bar{g} \quad \text{(A-54)}$$

$$K_{9,1}=-K_{9,13}=\sin\beta \quad \text{(A-55)}$$

$$K_{9,2}=-K_{9,14}=\cos\beta \quad \text{(A-56)}$$

$$K_{10,3}=-\rho^2\left(1-\bar{a}\right)\left(1-\overline{K}_b\right) \quad \text{(A-57)}$$

$$K_{10,13}=\overline{K}_b\sin\beta \quad \text{(A-58)}$$

$$K_{10,14} = \overline{K}_b \cos\beta \tag{A-59}$$

$$K_{10,15} = \overline{K}_b - \rho^2\left(1-\overline{a}\right)\left(1-\overline{K}_b\right) \tag{A-60}$$

$$K_{10,16} = \overline{K}_b \tag{A-61}$$

$$K_{11,1} = K_{13,13} = \rho^2 \sin\beta \tag{A-62}$$

$$K_{11,2} = K_{13,14} = \rho^2 \cos\beta \tag{A-63}$$

$$K_{11,6} = K_{13,10} = -\overline{\mu}\overline{g}\left(1-\overline{a}\right)^2 / \overline{b}^2 \tag{A-64}$$

$$K_{11,8} = K_{13,12} = \overline{\mu}\left(1-\overline{a}\right)^2 / \overline{b}^2 \tag{A-65}$$

$$K_{12,1} = -\overline{K}_{cL}\left(\frac{\sin\beta}{2} + \frac{\overline{a}\rho}{1-\overline{a}}\cos\beta\right) \tag{A-66}$$

$$K_{12,2} = \overline{K}_{cL}\left(-\frac{\cos\beta}{2} + \frac{\overline{a}\rho}{1-\overline{a}}\sin\beta\right) \tag{A-67}$$

$$-K_{12,3} = K_{12,5} = \overline{K}_{cL} \tag{A-68}$$

$$K_{12,6} = \overline{K}_{cL}\left[1 + \ln\overline{g} + \left(\frac{\overline{g}}{\overline{b}}\right)\left(1-\frac{\overline{g}}{\overline{b}}\right)\right] - \left(\frac{\overline{g}}{\overline{b}}\right)\left(1-\frac{\overline{g}}{\overline{b}}\right) \tag{A-69}$$

$$K_{12,8} = \overline{K}_{cL}\left[\left(\frac{1}{\overline{g}}\right) - \left(\frac{1}{\overline{b}}\right)\left(1-\frac{\overline{g}}{\overline{b}}\right)\right] + \left(\frac{1}{\overline{b}}\right)\left(1-\frac{\overline{g}}{\overline{b}}\right) \tag{A-70}$$

$$K_{14,9} = -K_{14,15} = \overline{K}_{cR} \tag{A-71}$$

$$K_{14,10} = \overline{K}_{cR}\left[1 + \ln\overline{g} + \left(\frac{\overline{g}}{\overline{b}}\right)\left(1-\frac{\overline{g}}{\overline{b}}\right)\right] - \left(\frac{\overline{g}}{\overline{b}}\right)\left(1-\frac{\overline{g}}{\overline{b}}\right) \tag{A-72}$$

$$K_{14,12} = \overline{K}_{cR}\left[\left(\frac{1}{\overline{g}}\right) - \left(\frac{1}{\overline{b}}\right)\left(1-\frac{\overline{g}}{\overline{b}}\right)\right] + \left(\frac{1}{\overline{b}}\right)\left(1-\frac{\overline{g}}{\overline{b}}\right) \tag{A-73}$$

$$K_{14,13} = -\overline{K}_{cR}\left(\frac{\sin\beta}{2} + \frac{\overline{a}\rho}{1-\overline{a}}\cos\beta\right) \tag{A-74}$$

$$K_{14,14} = \overline{K}_{cR}\left(-\frac{\cos\beta}{2} + \frac{\overline{a}\rho}{1-\overline{a}}\sin\beta\right) \tag{A-75}$$

$$K_{15,8} = K_{15,12} = K_{16,8} = -K_{16,12} = -1/\bar{b} \tag{A-76}$$

$$K_{16,6} = -K_{16,10} = 1 + \ln \bar{b} \tag{A-77}$$

For the shape factor n=3, the entries of the unknown constants' matrix are as follows:

$$K_{11,5} = K_{13,9} = K_{14,9} = K_{12,5} = K_{16,5} = K_{16,9} = 0 \tag{A-78}$$

$$K_{1,3} = K_{1,4} = K_{3,15} = K_{3,16} = K_{5,5} = K_{6,5} = K_{7,9} = K_{8,9} = K_{16,8} = -K_{16,11} = 1 \tag{A-79}$$

$$K_{1,1} = K_{3,13} = Y_{\bar{a},1} \tag{A-80}$$

$$K_{1,2} = K_{3,14} = J_{\bar{a},1} \tag{A-81}$$

$$K_{2,1} = Y_{\bar{a},1}\bar{a}\rho^2\left(1-\overline{K}_{fL}\right) + \overline{K}_{fL}\left(1-\bar{a}\right)\left(Y_{\bar{a},1} - \frac{\bar{a}\rho}{1-\bar{a}}Y_{\bar{a},0}\right) \tag{A-82}$$

$$K_{2,2} = J_{\bar{a},1}\bar{a}\rho^2\left(1-\overline{K}_{fL}\right) + \overline{K}_{fL}\left(1-\bar{a}\right)\left(J_{\bar{a},1} - \frac{\bar{a}\rho}{1-\bar{a}}J_{\bar{a},0}\right) \tag{A-83}$$

$$K_{2,3} = \overline{K}_{fL}\left(1-\bar{a}\right) \tag{A-84}$$

$$K_{4,13} = Y_{\bar{a},1}\bar{a}\rho^2\left(1-\overline{K}_{fR}\right) + \overline{K}_{fR}\left(1-\bar{a}\right)\left(Y_{\bar{a},1} - \frac{\bar{a}\rho}{1-\bar{a}}Y_{\bar{a},0}\right) \tag{A-85}$$

$$K_{4,14} = J_{\bar{a},1}\bar{a}\rho^2\left(1-\overline{K}_{fR}\right) + \overline{K}_{fR}\left(1-\bar{a}\right)\left(J_{\bar{a},1} - \frac{\bar{a}\rho}{1-\bar{a}}J_{\bar{a},0}\right) \tag{A-86}$$

$$K_{4,15} = \overline{K}_{fR}\left(1-\bar{a}\right) \tag{A-87}$$

$$K_{5,1} = K_{6,1} = K_{7,13} = K_{8,13} = -Y_1 \sin\alpha \tag{A-88}$$

$$K_{5,2} = K_{6,2} = K_{7,14} = K_{8,14} = -J_1 \sin\alpha \tag{A-89}$$

$$K_{5,3} = K_{6,3} = K_{7,15} = K_{8,15} = -\sin\alpha / \sqrt{\bar{a}} \tag{A-90}$$

$$K_{5,4} = K_{6,4} = K_{7,16} = K_{8,16} = -\sin\alpha\sqrt{\bar{a}} \tag{A-91}$$

$$K_{5,6} = K_{7,10} = \ln \bar{b} \tag{A-92}$$

$$K_{5,7} = K_{7,11} = \bar{b} \tag{A-93}$$

$$K_{5,8} = K_{7,12} = 1/\bar{b} \tag{A-94}$$

$$K_{6,6} = K_{8,10} = \ln \overline{g} \tag{A-95}$$

$$K_{6,7} = K_{8,11} = \overline{g} \tag{A-96}$$

$$K_{6,8} = K_{8,12} = 1/\overline{g} \tag{A-97}$$

$$K_{9,1} = -K_{9,13} = Y_1 \tag{A-98}$$

$$K_{9,2} = -K_{9,14} = J_1 \tag{A-99}$$

$$K_{9,3} = -K_{9,15} = 1/\sqrt{\overline{a}} \tag{A-100}$$

$$K_{9,4} = -K_{9,16} = \sqrt{\overline{a}} \tag{A-101}$$

$$K_{10,3} = -\rho^2\left(1-\overline{a}\right)\left(1-\overline{K}_b\right) \tag{A-102}$$

$$K_{10,13} = \overline{K}_b\sqrt{\overline{a}}Y_1 \tag{A-103}$$

$$K_{10,14} = \overline{K}_b\sqrt{\overline{a}}J_1 \tag{A-104}$$

$$K_{10,15} = \overline{K}_b - \rho^2\left(1-\overline{a}\right)\left(1-\overline{K}_b\right) \tag{A-105}$$

$$K_{10,16} = \overline{K}_b\,\overline{a} \tag{A-106}$$

$$K_{11,1} = K_{13,13} = \rho^2 Y_1 \tag{A-107}$$

$$K_{11,2} = K_{13,14} = \rho^2 J_1 \tag{A-108}$$

$$K_{11,6} = K_{13,10} = \overline{\mu}\,\overline{g}\left(1-\overline{a}\right)^2/\overline{b}^3 \tag{A-109}$$

$$K_{11,8} = K_{13,12} = -2\overline{\mu}\left(1-\overline{a}\right)^2/\overline{b}^3 \tag{A-110}$$

$$K_{12,1} = \overline{K}_{cL}\left(-Y_1 + \frac{\overline{a}^{\frac{3}{2}}\rho}{1-\overline{a}}Y_0\right) \tag{A-111}$$

$$K_{12,2} = \overline{K}_{cL}\left(-J_1 + \frac{\overline{a}^{\frac{3}{2}}\rho}{1-\overline{a}}J_0\right) \tag{A-112}$$

$$K_{12,3} = -\overline{K}_{cL}/\sqrt{\overline{a}} \tag{A-113}$$

$$K_{12,7} = \overline{K}_{cL} \tag{A-114}$$

$$K_{12,6}=\overline{K}_{cL}\left[\left(\frac{1}{\overline{g}}\right)-\left(\frac{\overline{g}}{\overline{b}^2}\right)\left(1-\frac{\overline{g}}{\overline{b}}\right)\right]+\left(\frac{\overline{g}}{\overline{b}^2}\right)\left(1-\frac{\overline{g}}{\overline{b}}\right) \tag{A-115}$$

$$K_{12,8}=\overline{K}_{cL}\left[\left(-\frac{1}{\overline{g}^2}\right)+\left(\frac{2}{\overline{b}^2}\right)\left(1-\frac{\overline{g}}{\overline{b}}\right)\right]-\left(\frac{2}{\overline{b}^2}\right)\left(1-\frac{\overline{g}}{\overline{b}}\right) \tag{A-116}$$

$$K_{14,10}=\overline{K}_{cR}\left[\left(\frac{1}{\overline{g}}\right)-\left(\frac{\overline{g}}{\overline{b}^2}\right)\left(1-\frac{\overline{g}}{\overline{b}}\right)\right]+\left(\frac{\overline{g}}{\overline{b}^2}\right)\left(1-\frac{\overline{g}}{\overline{b}}\right) \tag{A-117}$$

$$K_{14,11}=\overline{K}_{cR} \tag{A-118}$$

$$K_{14,12}=\overline{K}_{cR}\left[\left(-\frac{1}{\overline{g}^2}\right)+\left(\frac{2}{\overline{b}^2}\right)\left(1-\frac{\overline{g}}{\overline{b}}\right)\right]-\left(\frac{2}{\overline{b}^2}\right)\left(1-\frac{\overline{g}}{\overline{b}}\right) \tag{A-119}$$

$$K_{14,13}=-\overline{K}_{cR}\left(-Y_1+\frac{\overline{a}^{\frac{3}{2}}\rho}{1-\overline{a}}Y_0\right) \tag{A-120}$$

$$K_{14,14}=\overline{K}_{cR}\left(-J_1+\frac{\overline{a}^{\frac{3}{2}}\rho}{1-\overline{a}}J_0\right) \tag{A-121}$$

$$K_{14,15}=-\overline{K}_{cR}/\sqrt{\overline{a}} \tag{A-122}$$

$$K_{15,6}=K_{15,10}=K_{16,6}=-K_{16,10}=-1/\overline{b} \tag{A-123}$$

$$-K_{15,8}=-K_{15,12}=-2K_{16,8}=-2K_{16,12}=1/\overline{b}^2 \tag{A-124}$$

In these equations, the following non-dimensional parameters are assumed:

$$\rho^2=Pl_c^2/EI_c,\ \ \overline{\mu}=I_b/I_c,\ \ \overline{l}=l_b/l_c,\ \ \overline{a}=a/h,\ \ \overline{b}=b/h,\ \ \overline{g}=g/h,\ \ \overline{K}_{cL}=1/(1+EI_b/K_{cL}l_b),$$

$$\overline{K}_{cR}=1/(1+EI_b/K_{cR}l_b),\ \ \overline{K}_{fL}=1/(1+EI_c/K_{fL}l_c),\ \ \overline{K}_{fR}=1/(1+EI_c/K_{fR}l_c),\ \ \overline{K}_b=1/(1+EI_c/K_bl_c^3),$$

$$Y_{\overline{a},1}=BesselY\left(1,\frac{2\overline{a}\rho}{1-\overline{a}}\right),\ \ J_{\overline{a},1}=BesselJ\left(1,\frac{2\overline{a}\rho}{1-\overline{a}}\right),\ \ Y_{\overline{a},0}=BesselY\left(0,\frac{2\overline{a}\rho}{1-\overline{a}}\right),\ \ J_{\overline{a},0}=BesselJ\left(0,\frac{2\overline{a}\rho}{1-\overline{a}}\right),$$

$$Y_1=BesselY\left(1,\frac{2\overline{a}^{\frac{3}{2}}\rho}{1-\overline{a}}\right),\ \ J_1=BesselJ\left(1,\frac{2\overline{a}^{\frac{3}{2}}\rho}{1-\overline{a}}\right),\ \ Y_0=BesselY\left(0,\frac{2\overline{a}^{\frac{3}{2}}\rho}{1-\overline{a}}\right),\ \ J_0=BesselJ\left(0,\frac{2\overline{a}^{\frac{3}{2}}\rho}{1-\overline{a}}\right),$$

$$\beta=\sqrt{\left(\frac{\overline{a}\rho}{1-\overline{a}}\right)^2-\frac{1}{4}}\times\ln\left(\frac{1}{\overline{a}}\right).$$